ULTIMATE STRENGTH ANALYSIS OF BEAMS WITH ECCENTRIC RECTANGULAR WEB OPENINGS

by

MICHAEL WAYNE RICHARD

B. S., United States Military Academy, 1964
B. S., Kansas State University, 1970

5248

A MASTER'S THESIS

submitted in partial fulfillment of the

requirements for the degree

MASTER OF SCIENCE

Department of Civil Engineering

KANSAS STATE UNIVERSITY
Manhattan, Kansas

1971

Approved by:

Peter B. Cooper
Major Professor

LD
2668
T4
1971
R52
c.2

ABSTRACT

A new analytical method of determining the moment carrying capacity of beams with eccentric rectangular web openings is developed. Using this method, the effects of varying the opening eccentricity, length and height were investigated analytically for a number of beam sections. From this analysis, the following conclusions are drawn: a. As opening eccentricity increases, the moment carrying capacity decreases for low shear values and increases for high shear values; b. As opening length increases, the moment carrying capacity decreases; c. As opening height increases, the moment carrying capacity decreases; d. As opening length becomes successively smaller than opening height, the moment carrying capacity increases; e. Shear forces are unequally distributed across unequal web areas above and below eccentric openings. The larger area carries the larger shear force.

The analytical results compared favorably with the limited experimental data available. In all cases, the analytical results were slightly conservative.

TABLE OF CONTENTS

Chapter		Page
	ABSTRACT	ii
I.	INTRODUCTION	1
	1.1 Problem Statement	1
	1.2 Literature Review	2
	1.3 Scope of the Investigation	4
II.	ULTIMATE STRENGTH ANALYSIS	5
	2.1 Assumptions	5
	2.2 General Approach	7
	2.3 Analysis	8
	a. Case I	9
	b. Case II	14
	c. Case III	16
	2.4 Computer Program	19
III.	INVESTIGATION OF VARIABLES	22
	3.1 General Tests	22
	3.2 Specific Tests	22
IV.	DISCUSSION OF RESULTS	23
	4.1 General Results	23
	4.2 Specific Results	25
V.	CONCLUSIONS	27
VI.	RECOMMENDATIONS FOR FURTHER STUDY	28
	FIGURES AND TABLES	29
	APPENDIX A Nomenclature	56

APPENDIX B Computer Program 59

APPENDIX C Computer Print-out 67

REFERENCES 68

ACKNOWLEDGEMENTS 70

CHAPTER I

INTRODUCTION

1.1 Problem Statement

The primary problem with which the structural designer is faced is that of designing safe, functional structures while maintaining material and labor costs as low as possible. Many standard design procedures are based upon such an economic principle.

In the case of multi-story building design, economic principles are of paramount importance. All other variables being equal, the design which results in the lowest structure will be the most economical and desirable design. This is logical when one considers the additional materials and labor required to increase the height of such a structure. Comfortable human occupation demands that the floor to ceiling height in such a structure be relatively fixed. Thus, the distance from the floor of one story to the ceiling of the story below becomes a critical distance which must be minimized to insure minimum overall building height.

One procedure which has proved very satisfactory in this regard is to cut rectangular holes in the webs of girders to allow for the passage of heating and air-conditioning ducts. Prior to this practice, ductwork had been placed either above or below the girders, which increased the between floor distance by the height of the particular duct. The practice of passing ducts thru the webs of the girders resulted partially from analytical and experimental investigations of the effects produced when rectangular and other shaped openings were present in the webs of beams (A synopsis of this work will be found in Section 1.2). All of this work, however, concerned openings

which were centered on the middepth of the beams. As far as can be determined, no analytical work and very little experimental work has been carried out to determine the effect of locating web openings off the middepth of the beam. Yet, returning to the multi-story building design, it is not difficult to imagine that within any particular floor system, several different sizes of girders may be used. The designer, being restricted to using center line web openings only, would have to sacrifice much of the material and labor savings by being forced to have all of the ductwork curved and twisted to fit the center cut openings of the various sized girders. A more economical solution would be to allow the ductwork to remain straight and to vary the location of the openings in the various sized girders to allow for the passage of straight ducts. After all, it should cost no more to cut an opening off center than to cut the same opening in the center of a beam web.

Prior to adopting such a procedure, however, the resulting loss of strength and moment carrying capacity must be known and allowed for in the design. It is obvious that some change in behavior and stress distribution must occur when the opening is cut off center as opposed to being cut in the center of the web. The basic question is exactly how much change will occur and in which direction? The answer to this question from an analytical point of view forms the basis of this thesis. An ultimate strength analytical solution to the problem of eccentric web openings will be presented, verified and discussed in the pages which follow.

1.2 Literature Review

The subject of openings in the webs of wide flange beams has received considerable attention in recent literature. Much work has been conducted

analyzing the stresses around such openings utilizing the elastic theory (1, 2,3,4). Ultimate strength behavior of such beams has been the subject of recent papers. One paper (5) presented an ultimate strength analysis in which the effects of secondary bending were not included. Two other papers (6,7) concerned experimental investigations, the test results of which were not correlated with an ultimate strength analysis.

In 1968, Bower (8) conducted an ultimate strength analysis of rectangular openings in the webs of beams. His theory was based upon the assumption that a point of contraflexure occurred above and below the center of the opening. Experimental results were not correlated with the theory because of the effect of strain hardening.

Also in 1968, Redwood (9) conducted an ultimate strength analysis of the same problem. His theory differed from Bower's insofar as the points of contraflexure were assumed to occur somewhere along the length of the opening, not necessarily in the center. Correlation with previous experimental work indicated the theoretical results were conservative when shears were large. A subsequent paper (10) partially rectified this situation, which was caused primarily by the effects of strain hardening.

Reinforced rectangular openings were analyzed by Congdon in 1969 (11). Experimental results were correlated with the theory and an approximate method of analysis was offered.

In all of the papers thus far discussed, the center lines of the openings coincided with the longitudinal center lines of the beams. No theoretical analysis has been found which treats the subject of eccentric openings. The limited experimental work in this area has been conducted by U. S. Steel Corporation (12,13).

1.3 Scope of the Investigation

This investigation was limited to an analytical, ultimate strength analysis of wide flange beams containing unreinforced, rectangular, eccentric openings in their webs. Variables investigated included moment to shear ratios, opening lengths, opening depths and opening eccentricities. The shear distribution across the unequal web areas above and below eccentric openings was also investigated, but to a somewhat limited extent.

CHAPTER II

ULTIMATE STRENGTH ANALYSIS

2.1 Assumptions

For the purpose of this analysis, several assumptions were made which simplified and indeed made possible some of the necessary calculations. These assumptions will be outlined and discussed.

a. Failure of the member occurs through the formation of a four hinge mechanism, each hinge being located at a corner of the opening. The beam, opening and assumed mechanism is shown in Fig. 1(a) while a cross section through the opening is shown in Fig. 1(b).

b. Points of contraflexure occur in the centers of the tee sections above and below the opening. This assumption will permit the calculation of secondary bending due to shear. The secondary bending moment concept will best be understood by referring to Fig. 2. This illustration shows the forces acting on the beam at a section through the mid length of the opening. Note that the shear forces V_t and V_b acting on the ends of the tee sections induce moments at sections two and four respectively, in much the same manner as a concentrated load at the end of a cantilever beam induces a moment at the fixed end. These moments induced by the shear forces will be referred to as secondary moments. All moments which are not attributed to nor required to resist the transverse shear forces will be referred to as primary moments.

c. Assumed stress distributions for sections one thru four are indicated in figures 3(a) thru 3(d) respectively. At sections one and three, the point of stress reversal may occur either in the web or in the flange. At sections two and four, it is assumed that the point of stress reversal

will always occur in the flange.

d. For any of the four sections, that portion of the stress distribution diagram which results from secondary bending is balanced by an equal portion from the opposite stress distribution. It is assumed that the balancing portion is taken from the extreme opposite end of the stress diagram, to achieve the maximum lever arm to resist the secondary moment. Referring to Fig. 4, the indicated positive portion of the stress diagram must be balanced by a portion of the negative distribution. According to this assumption, the balancing portion is taken from the extreme opposite end, indicated by the crosshatched area. The remaining negative portion of the stress distribution diagram contributes to resisting the primary moment.

e. Shear stresses are assumed to be carried only by the webs of the tee sections above and below the opening. It is further assumed that these stresses are uniformly distributed over the depth of the respective web segments.

f. Yielding in the flanges is in direct tension or compression. Yielding in the web occurs under combined bending and shear and is governed by the Von Mises' yield criteria (14).

g. As the shear force increases, the point of stress reversal at section one will enter the flange before the point of stress reversal at section three enters the flange. This assumption is based on the fact that for eccentric openings, the web area at section one will be less than the web area at section three.

For the purpose of this analysis, the opening will always be displaced toward the top (or compression) flange of the beam. Eccentricity in that direction will be considered positive eccentricity and all derivations and

examples will be based on positive eccentricity. However, should an opening with negative eccentricity be encountered, the shape of the interaction curve will be exactly the same as the one for the same specimen and opening with positive eccentricity. This result will apply as long as the yield stress of the beam is the same in tension as in compression.

2.2 General Approach

Prior to discussing in detail the method of solution and the derivation of all equations, it is felt that the reader will benefit from knowing the general, overall approach which was used to solve the problem. To accomplish this purpose, a flow diagram of the basic steps used in arriving at a solution has been included (see Fig. 5). The basic procedure shown is applicable to all cases of stress reversal. Only the equations used to determine the indicated parameters change. The reader will be able to follow the flow diagram as the detailed method of solving the problem is discussed in the following pages.

One problem which was encountered was the distribution of shear forces across unequal web areas above and below an eccentric opening. Nowhere in the literature could an exact procedure be found for the correct distribution of such forces. In one paper (12), Bower summarized five different approaches for distributing such forces. However, experimental results compared favorably with only one approach. It was recommended that this approach be used when applying the Vierendeel analysis which for the purposes of this ultimate strength analysis, would not be applicable.

The problem was solved by assuming a shear force across the top tee section. Then, thru application of static equilibrium principles and the

Von Mises' yield criteria, a shear force was determined across the bottom tee section which satisfied these criteria. This procedure will be illustrated and discussed in subsequent pages.

Considering assumptions c and g, three different stress reversal cases were developed considering all sections acting together. These cases were designated as follows:

Case	Section	Stress Reversal in:
I	1	Web
	2	Flange
	3	Web
	4	Flange
II	1	Flange
	2	Flange
	3	Web
	4	Flange
III	1	Flange
	2	Flange
	3	Flange
	4	Flange

Derivations and discussion for each case will be treated separately from the other cases.

2.3 Analysis

Throughout this section, the symbols used in the derivation of equations are defined where they first appear, in either the illustrations or

the text. In addition, Appendix A contains a listing of all symbols with the appropriate definitions.

a. Case I

The shear force V_t across the top tee section is assumed and varies from a small finite amount up to the maximum amount which the section can carry.

Knowing the shear force across the top tee section, the shear stress is determined from assumption e:

$$\tau_t = \frac{V_t}{w(s - e)} \tag{1}$$

Knowing the shear stress, the normal stress carrying capacity of the web is determined from the Von Mises' yield criteria (14). A simplification of this criteria as it applies to a biaxial state of stress may be expressed mathematically as follows:

$$\sigma_y^2 = \sigma_n^2 + 3\tau^2 \tag{2}$$

where σ_y is the yield stress, σ_n is the normal stress carrying capacity and τ is the shear stress. Rewriting for the top tee section:

$$\sigma_y^2 = \sigma_t^2 + 3\tau_t^2 \tag{3}$$

or

$$\sigma_t^2 = \sigma_y^2 - 3\tau_t^2 \tag{4}$$

σ_t and τ_t are respectively the normal stress and the shear stress acting on

the top tee section. The secondary moment caused by the shear force V_t may be computed from equilibrium:

$$M_1 = (V_t)(a) \tag{5}$$

where M_1 is the secondary moment at section one and a is the half length of the opening.

Referring to Fig. 6, the resisting secondary moment is calculated from the stress distribution diagram.

$$F_+ = k_1(s - e)(\sigma_t)(w) \tag{6}$$

$$F_{ch} = g_1(\sigma_y)(b) \tag{7}$$

From equilibrium, these two forces must be equal. Equating and solving for g_1 yields:

$$g_1 = \frac{k_1(s - e)(\sigma_t)(w)}{(\sigma_y)(b)} \tag{8}$$

The distance between the two forces is the moment arm and the expression for this distance is:

$$\text{Moment Arm} = (s - e) + t - \frac{g_1}{2} - \frac{k_1(s - e)}{2} \tag{9}$$

The g_1 term is eliminated by substituting Eqn. 8 into Eqn. 9. The internal resisting secondary moment is then determined from:

$$M_1 = (F_+)(\text{Moment Arm}) \tag{10}$$

Substituting Eqns. 6 and 9 into Eqn. 10 and equating the resulting expression

to M_1 determined from Eqn. 5, the following quadratic equation is obtained:

$$k_1^2\left[\frac{(s-e)^2\sigma_t w}{2}\left(\frac{\sigma_t w}{\sigma_y b}+1\right)\right]-k_1[\sigma_t w(s-e)(s-e+t)]+V_t a=0 \quad (11)$$

Eqn. 11 is solved for k_1. Only one root satisfies the location of the point of stress reversal assumed for Case I ($0<k_1<1.0$).

Knowing k_1, the overall force at section one is determined from the stress distribution diagram:

$$F_1 = A_f\sigma_y + \sigma_t w(s-e)(1-2k_1) \quad (12)$$

Referring to Fig. 7(a), equilibrium of the top tee section requires that $F_1 = F_2$. From the stress distribution diagram, the force at section two is:

$$F_2 = (s-e)w\sigma_t + A_f\sigma_y(1-2k_2) \quad (13)$$

Knowing F_2, Eqn. 13 is solved for k_2. To satisfy stress reversal requirements, $0<k_2<1.0$.

Referring to Fig. 7(b), equilibrium requires that $F_1 = F_3$. From the stress distribution diagram for section three:

$$F_3 = A_f\sigma_y + \sigma_b w(s+e)(1-2k_3) \quad (14)$$

Knowing F_3, the only unknown terms in Eqn. 14 are σ_b, the normal stress carrying capacity of the bottom tee section and k_3, the location of stress reversal at section three. The equation is solved for k_3 in terms of σ_b, resulting in:

$$k_3 = \frac{1}{2} - \frac{F_3 - A_f\sigma_y}{2w(s + e)\sigma_b} \tag{15}$$

In the same manner as for the top tee section, secondary moment relationships can be determined for the bottom tee section. For any shear force V_b assumed across the bottom tee section, the shear stress will be from assumption e:

$$\tau_b = \frac{V_b}{w(s + e)} \tag{16}$$

From the Von Mises' yield criteria, the normal stress carrying capacity is:

$$\sigma_b^2 = \sigma_y^2 - 3\tau_b^2 \tag{17}$$

The secondary moment expression for section three derived from the stress distribution diagram is:

$$M_3 = k_3(s + e)w\sigma_b[(s + e) + t - \frac{k_3(s + e)}{2}(\frac{w\sigma_b}{b\sigma_y} + 1)] \tag{18}$$

Likewise, the secondary moment produced by the shear force across the bottom tee section is:

$$M_3 = (V_b)(a) \tag{19}$$

For any given value of V_b, Eqn. 18 must equal Eqn. 19. Eqn. 15 must also be satisfied because of the equilibrium condition that $F_1 = F_3$. One way of solving these three equations is by trial and error. Assuming a shear force V_b, the normal stress capacity σ_b is determined from Eqns. 16 and 17. k_3 is then determined from Eqn. 15. Knowing k_3, Eqn. 18 is solved for the

secondary moment M_3. This is compared to the secondary moment found from Eqn. 19 and if the two are unequal, V_b is incremented and the process repeated until a value of V_b is found which results in the secondary moment expressions being, for all practical purposes, equal.

Using the values of V_b and σ_b which satisfy all equations, k_3 is known from Eqn. 15 and is checked to insure that the stress reversal assumptions for Case I are satisfied ($0<k_3<1.0$). From equilibrium of the bottom tee section, $F_3 = F_4$. The force expression for section four is determined from the stress distribution diagram:

$$F_4 = \sigma_b w(s + e) + A_f\sigma_y(1 - 2k_4) \tag{20}$$

k_4 may be determined using Eqn. 20 and must be checked to insure that k_4 is less than 1.0.

Knowing all of the locations of stress reversal, the forces on the sections and the normal stress carrying capacities for any given value of shear, the moment capacity at the mid length of the opening can be determined. Referring to Fig. 8, the moment at the opening mid length is determined as follows:

$$\Sigma M_x = 0$$

$$F_2(y_2 + h) + F_4(y_4 + h) - V\ell + Va = 0 \tag{21}$$

But, the moment at the center is $V\ell$. Thus:

$$M = F_2(y_2 + h) + F_4(y_4 + h) + Va \tag{22}$$

From the stress diagrams of sections two and four, the following equations are derived for F_2y_2 and F_4y_4:

$$F_2 y_2 = \frac{1}{2} w\sigma_t (s - e)^2 + A_f \sigma_y [(s - e)(1 - 2k_2) + \frac{t}{2}(2k_2^2 - 4k_2 + 1)] \quad (23)$$

$$F_4 y_4 = \frac{1}{2} w\sigma_b (s + e)^2 + A_f \sigma_y [(s + e)(1 - 2k_4) + \frac{t}{2}(2k_4^2 - 4k_4 + 1)] \quad (24)$$

Equations for F_2 and F_4 have already been designated as Eqns. 13 and 20, respectively. Thus, all terms being known, Eqn. 22 is solved for the moment capacity at the mid length of the opening.

b. Case II

The same basic procedure used to develop Case I is used for Case II. The only difference is that stress reversal at section one occurs in the flange. Thus, a different formula has to be developed with which k_1 can be determined.

For an assumed value of shear across the top, the normal stress capacity is determined as in the previous section. With the stress reversal occurring in the flange at section one however, the secondary moment expression derived from the stress distribution diagram changes. Referring to Fig. 9, the secondary moment relationships are:

$$F_+ = (s - e)w\sigma_t + (t - k_1 t)b\sigma_y \quad (25)$$

$$F_{ch} = g_1 \sigma_y b \quad (26)$$

Since from equilibrium the two forces must be equal, Eqns. 25 and 26 are solved for g_1:

$$g_1 = \frac{(s - e)w\sigma_t}{b\sigma_y} + t(1 - k_1) \quad (27)$$

From the top of the flange, the centroid of F_+ is:

$$y = \frac{(s - e)w\sigma_t\left(t + \frac{s - e}{2}\right) + (t - k_1 t)b\sigma_y\left(t - \frac{t - k_1 t}{2}\right)}{(s - e)w\sigma_t + (t + k_1 t)b\sigma_y} \tag{28}$$

The distance between F_+ and F_{ch} is the internal secondary resisting moment arm and can be expressed as:

$$\text{Moment Arm} = y - \frac{g_1}{2} \tag{29}$$

Substituting Eqn. 27 into Eqn. 29 eliminates the g_1 term. The equation for the internal secondary resisting moment is:

$$M_1 = (F_+)(\text{Moment Arm}) \tag{30}$$

Substituting Eqns. 25, 29 and 28 in Eqn. 30 and equating the resulting expression to M_1 determined from Eqn. 5, the following quadratic equation is obtained:

$$k_1^2 A_f t\sigma_y - k_1[A_f\sigma_y t + t(s - e)w\sigma_t] - \frac{(s - e)^2 w\sigma_t}{2}\left(1 - \frac{w\sigma_t}{b\sigma_y}\right) + V_t a = 0 \tag{31}$$

Solution of the above quadratic equation gives k_1, the point of stress reversal at section one. Only one solution to the quadratic equation satisfies the stress reversal assumption ($0<k_1<1.0$).

Knowing k_1, the force on the section is determined from the following formula which was derived from the Case II stress distribution diagram for section one:

$$F_1 = A_f\sigma_y(2k_1 - 1) - (s - e)w\sigma_t \tag{32}$$

The determined values of k_1 and F_1 are used throughout the remainder of the calculations exactly as was done in Case I. This procedure is valid for increasing values of shear until the stress reversal at section three goes from the web into the flange. At that time, Case III begins and some of the calculations have to again be revised.

c. Case III

As in Case II, the same basic procedure is used to develop Case III as was used to develop Case I. The only difference from Case II is that stress reversal at section three is in the flange instead of the web.

For the assumed value of shear across the top tee section, the same procedure for determining shear stress, normal stress capacity, k_1, k_2 and F_1 is followed as for Case II. Secondary moment relations for section three are changed to reflect the changed stress reversal location. Referring to Fig. 10, the following relationships are derived from the stress distribution diagram:

$$F_- = (s + e)w\sigma_b + (t - k_3 t)b\sigma_y \tag{33}$$

$$F_{ch} = g_3\sigma_y b \tag{34}$$

From equilibrium, the above two forces must be equal. Solving Eqns. 33 and 34 for g_3 yields:

$$g_3 = \frac{(s + e)w\sigma_b}{b\sigma_y} + t - k_3 t \tag{35}$$

From the bottom of the flange, the centroid of F_- is:

$$y = \frac{(s + e)w\sigma_b(t + \frac{s + e}{2}) + (t - k_3t)b\sigma_y(t - \frac{t - k_3t}{2})}{(s + e)w\sigma_b + (t - k_3t)b\sigma_y} \tag{36}$$

The distance between F_- and F_{ch} is the internal resisting secondary moment arm. The expression for this distance is:

$$\text{Moment Arm} = y - \frac{g_3}{2} \tag{37}$$

Substituting Eqn. 35 into Eqn. 37 eliminates the term g_3. The internal resisting secondary moment is determined from the equation:

$$M_3 = (F_-)(\text{Moment Arm}) \tag{38}$$

Substituting Eqns. 33, 37 and 36 into Eqn. 38 results in the following secondary moment expression:

$$k_3^2A_ft\sigma_y - k_3(A_f\sigma_yt + t(s + e)w\sigma_b) - \frac{(s + e)^2w\sigma_b}{2}(1 - \frac{w\sigma_b}{b\sigma_y}) = M_3 \tag{39}$$

From the stress distribution diagram, the following expression for the force on section three is derived:

$$F_3 = A_f\sigma_y(2k_3 - 1) - (s + e)w\sigma_b \tag{40}$$

Knowing F_1 and that $F_1 = F_3$, Eqn. 40 is solved for k_3 for any assumed value of shear across the bottom. Knowing k_3, Eqn. 39 is solved for the resisting secondary moment. The secondary moment M_3 determined from Eqn. 19 is compared to the resisting moment determined from Eqn. 39 and if the two are unequal, V_b is changed in the appropriate direction and the iteration process is

repeated until the two secondary moment values are, for all practical purposes, equal. At that time, the value of k_3 is checked to insure that $0<k_3<1.0$. Knowing that $F_3 = F_4$, the value of k_4 is determined from the following equation derived from the stress distribution diagram:

$$k_4 = 1 - k_3 + \frac{w\sigma_b(s + e)}{A_f\sigma_y} \tag{41}$$

k_4 is then checked to insure that the stress reversal assumption was satisfied, that is, $0<k_4<1.0$. The value of the moment at the mid length of the opening is determined in the same manner as in Case I.

One peculiarity of this method of analysis is the inability to calculate the moment capacity for zero shear. This is because, even with zero shear assumed across the top tee section, there was always some shear calculated across the bottom section. It has been concluded that for very small values of shear, the portion carried by the top (or smaller) section is negligible until a certain value is reached, at which time both sections begin to carry significant portions of the shear force. Thus, the values of moments for zero shear are calculated from the expressions which follow:

for zero eccentricity:

$$M_{pi} = 2\sigma_y A_f(s + h + \frac{t}{2}) + 2A_w\sigma_y(\frac{s}{2} + h) \tag{42}$$

for non zero eccentricity:

$$M_{pi} = A_f\sigma_y(d - t) + w\sigma_y[sd - s^2 - 2st + e(2s - d + 2t)] \tag{43}$$

Utilizing the procedures set forth in this chapter, moment carrying capacities for varying values of shear forces were computed. This data was plotted graphically in the form of interaction curves. Prior to plotting

however, the calculated moments and the assumed shear forces were nondimensionalized by division by the plastic moment and shear capacities of the uncut sections. The equations for these values follow:

$$M_p = A_f\sigma_y(d - t) + w(d - 2t)^2 \frac{\sigma_y}{4} \tag{44}$$

$$V_p = \frac{w(d - 2t)\sigma_y}{\sqrt{3}} \tag{45}$$

The maximum shear or shear limit is the ratio of the web area of the cut section to the web area of the uncut section:

$$V_\ell = \frac{d - 2t - 2h}{d - 2t} V_p \tag{46}$$

The computed shear value cannot ever exceed the above limit. It was found that for the unreinforced openings investigated analytically, the strength of the member was always controlled by the moment carrying capacity at the opening. Thus, the shear limit given by Eqn. 46 did not control the solution in any of these cases.

2.4 Computer Program

A computer program was developed to compute interaction curves for any combination of beam and opening sizes and eccentricities, using the formulas and procedures discussed in section 2.3. Several modifications were made to the basic procedure, however, to insure continuity of the resultant interaction curve.

It was found that for eccentric openings, practically all of the

initial shear force increments are carried by the larger web section only. The shear force across the smaller web section remained insignificant until a higher value of total, applied shear was reached. Therefore, assuming a significant value of V_t for the initial increment sometimes could, and in fact did, result in interaction curves with no plotted points for low shear values up to 60% of the range of the shear ordinate. In addition, referring to Fig. 11, the M/M_p value corresponding to zero shear seemed inconsistent with the remaining shape of the interaction curve. In the figure, the dashed line indicates the curve shape which would seem more reasonable, while the solid line indicates the shape required to intersect the moment axis at the computed maximum moment value. To verify the seemingly inconsistent shape of the interaction curve, the bottom shear force corresponding to a negligible (V_t = 0.00005) value of top shear was determined. Then several approximate points were determined within the interval to confirm the shape of the interaction curve. The additional points did confirm the seemingly inconsistent decrease in moment capacity for low values of shear.

To insure continuity from Case I to Case II, the program was modified to compute a point at the exact shear value where the stress reversal changes (at k_1 = 1.0). This procedure also facilitated a more uniform point spread through the range of Case II.

The program has been designed to print out all data needed to independently check any particular values. The method used by the author to check the calculations was to compute the primary moments at sections 1-3 and 2-4 from the stress distribution diagrams. Only those portions of the diagrams not used in balancing the secondary moments were used to calculate the primary moments. The difference between the primary moments at sections

1-3 and 2-4 should equal zero and both should equal the computed moment value at the mid length of the opening.

The computer program is reproduced in Appendix B. A sample print out of results will be found in Appendix C.

CHAPTER III

INVESTIGATION OF VARIABLES

3.1 General Tests

Beam sizes, opening dimensions and eccentricities were selected to gain insight into the effects induced by changing various parameters. In particular, the parameters were:

a. Increasing eccentricity

b. Increasing opening length

c. Increasing opening height

d. Height of opening greater than length

Six beam sizes were selected from the allowable stress design beam selection table in the AISC Steel Construction Manual (15). These beams are the most economical for a particular range of section modulus values, since these would be the most commonly used sections in actual practice.

Table 1 indicates the various beam and opening dimensions used for the first seven tests. Two tests with different beam sizes were conducted for the first three parameters investigated, while one test was conducted for the last parameter. The interaction curves derived from this data indicate general trends resulting when the indicated parameters are varied as shown.

3.2 Specific Tests

Specific examples were also calculated in order to compare results with the limited experimental results available (13). The data is summarized in Table 2. Test F was conducted in order to compare the theoretical values of shear distribution across eccentric openings with experimental results (12).

CHAPTER IV

DISCUSSION OF RESULTS

4.1 General Results

The interaction curves derived for the general tests are shown in Figs. 12 thru 18. The results will be discussed separately.

Figures 12 and 13 show how the moment capacity changes with varying eccentricity. As indicated by the figures, when eccentricity is increased, the moment carrying capacity also increases for the higher values of shear. However, it is evident that for lower values of shear, the moment capacity decreases below that for zero eccentricity. Although the change is small in comparison to the size of the change in eccentricity, the fact that the change may go in either direction is significant. The reason for the decrease for low shear values is that the maximum normal force on either tee section is limited to that which the smaller tee section is capable of withstanding. The increase in the strength of beams with eccentric openings subjected to high shear forces is due to an increase in the moment arms in the larger tee section which is greater than the decrease in moment arms in the smaller tee section.

Figures 14 and 15 show the interaction curves produced when a change in opening length occurs. As can be seen, the moment carrying capacity decreases as the opening length increases. This is understandable insofar as the secondary moment to be resisted increases as the opening length and thus the moment arm for the shear forces increases.

Figures 16 and 17 show that as the depth of the opening increases, the moment carrying capacity decreases. As opening depth increases, web area

decreases. Thus, less normal force capacity exists for any value of shear, and the moment carrying capacity is reduced.

In the above two tests, two samples were included in each test. One sample had an eccentricity of zero, while the other had some eccentricity. Comparison of the respective graphs indicates that the general results discussed are applicable to both the concentric and eccentric openings. Closer observation also confirms the characteristics previously indicated as being associated with eccentric openings as compared with concentric openings. That is, with eccentric openings, the interaction curves tend to flatten out for low values of shear, thereby decreasing the moment carrying capacity. For higher values of shear, the moment carrying capacity tends to increase.

The results of the last general test are shown in Fig. 18. The objective was to investigate the consequences of the opening length becoming successively smaller than the opening depth. As shown in the interaction curve, the moment capacity increases. This is due to the moment arm for the shear forces decreasing, thereby decreasing the secondary moments which the sections must resist.

During the testing of the various beams, openings and eccentricities, it was noted that several of the initial assumptions made in section 2.1 held true for all combinations of variables. Specifically, assumption c concerning the points of stress reversal always proved to be correct. That is, the points of stress reversal at sections two and four always remained in the flanges while the points of stress reversal at sections one and three occurred in both the web and the flanges. Assumption g was also verified as being correct. The point of stress reversal at section one always entered

the flange before the point of stress reversal at section three.

4.2 Specific Results

Figures 19 thru 22 indicate the correlation between the available experimental results (13) and the computed analytical results. The interaction curves have been plotted using data generated from the computer analysis. On each graph is plotted the experimental point obtained for the indicated value of moment to shear ratio. The dashed lines indicate the interaction curve obtained using the same beam and opening with zero eccentricity. It will be noted that in all cases, the analytical result gives a more accurate prediction of the ultimate strength than the concentric (or zero eccentricity) result. However, even the analytical results were slightly conservative when compared to the experimental results. This indicates that the analytical results provide a reasonable, but somewhat conservative estimate of the actual strength of beams with eccentric web openings.

The last test consists of a comparison of the shear force distributions across the unequal tee sections. The results are presented in Table 3, and indicate that the analytical results compared quite favorably with the results obtained experimentally. In fact, the correlation is better than any of the analytical methods thus far proposed (12).

It has been suggested that opening eccentricity will result in little change from the concentric hole case (13). The results of this study indicate that for small values of eccentricity, this statement is correct. However, as eccentricity is increased, the change becomes more pronounced and more importantly, for low values of shear the moment carrying capacity is less

than that for the concentric case. For higher values of shear, the moment capacity increases which would make the concentric case a more conservative solution.

CHAPTER V

CONCLUSIONS

A new analytical method has been developed to determine the ultimate moment capacity of wide flange beams containing eccentric rectangular web openings.

Comparison with the limited experimental results available indicates that the analytical method of analysis presented herein provides a reasonably accurate prediction of the moment carrying capacity for any given combination of beam size, opening size and eccentricity.

Based on the discussion and results of the previous chapter, the following specific conclusions can be formulated:

a. As the opening eccentricity increases, the moment carrying capacity increases for high values of shear and decreases for low values of shear.

b. As the length of an eccentric (or otherwise) opening increases, the moment carrying capacity will decrease.

c. As the height of an eccentric (or concentric) opening increases, the moment carrying capacity will decrease.

d. If the opening length becomes successively smaller than the height, the moment carrying capacity will increase.

e. Shear forces across an eccentric opening are distributed unequally, with the larger web area carrying the larger portion of the shear force.

CHAPTER VI

RECOMMENDATIONS FOR FURTHER STUDY

Following the present analysis, the logical next step would be to conduct a similar analysis for reinforced eccentric openings. Basically, the same procedures discussed in this paper could be applied to the reinforced opening case. The significant difference would be the existence of several additional cases of stress reversal. For sections one and three, cases would have to be developed to handle stress reversals in the reinforcing, above and below the reinforcing and in the flanges. With the eccentric opening, almost any combination of stress reversals in sections one and three may be possible, and provisions would have to be made to check the locations of stress reversals and to apply the correct procedures for each case.

Experimental study of eccentric web openings would also be appropriate so that correlation between the analytical and experimental results would be more accurate and meaningful. Experimental programs should include unreinforced as well as reinforced eccentric web openings.

Test	Beam	No.	d	b	t	w	2h/d	2h	a/h	2a	e/d	e
A1	W14x26	1	13.89	5.025	0.418	0.244	0.4	5.556	2.0	11.112	0.00	0.0000
		2	"	"	"	"	"	"	"	"	0.05	0.6945
		3	"	"	"	"	"	"	"	"	0.10	1.3890
		4	"	"	"	"	"	"	"	"	0.15	2.0835
		5	"	"	"	"	"	"	"	"	0.20	2.7780
A2	W24x76	6	23.91	8.985	0.682	0.440	0.4	9.564	2.0	19.128	0.00	0.0000
		7	"	"	"	"	"	"	"	"	0.05	1.1955
		8	"	"	"	"	"	"	"	"	0.10	2.3910
		9	"	"	"	"	"	"	"	"	0.15	3.5865
		10	"	"	"	"	"	"	"	"	0.20	4.7820
B1	W12x22	11	12.31	4.030	0.424	0.260	0.5	6.155	1.5	9.2325	0.00	0.0000
		12	"	"	"	"	"	"	2.0	12.3100	"	"
		13	"	"	"	"	"	"	2.5	15.3875	"	"
		14	"	"	"	"	"	"	3.0	18.4650	"	"

Note: Yield Stress for Flanges and Webs Assumed 36.0 ksi

Table 1 : Beam and Opening Data - General Tests

Test	Beam	No.	d	b	t	w	2h/d	2h	a/d	2a	e/d	e
B2	W21x44	15	20.66	6.500	0.451	0.348	0.5	10.330	1.5	15.4950	0.10	2.0660
		16	"	"	"	"	"	"	2.0	20.6600	"	"
		17	"	"	"	"	"	"	2.5	25.8250	"	"
		18	"	"	"	"	"	"	3.0	30.9900	"	"
C1	W30x99	19	29.64	10.458	0.670	0.522	0.1	2.964	1.5	17.784	0.00	0.0000
		20	"	"	"	"	0.2	5.928	"	"	"	"
		21	"	"	"	"	0.3	8.892	"	"	"	"
		22	"	"	"	"	0.4	11.856	"	"	"	"
C2	W18x35	23	17.71	6.000	0.429	0.298	0.1	1.771	1.5	10.626	0.20	3.5420
		24	"	"	"	"	0.2	3.542	"	"	"	"
		25	"	"	"	"	0.3	5.313	"	"	"	"
		26	"	"	"	"	0.4	7.084	"	"	"	"
D	W24x61	27	23.72	7.023	0.591	0.419	0.5	11.860	1.0	11.860	0.10	2.3720
		28	"	"	"	"	"	"	0.8	9.488	"	"
		29	"	"	"	"	"	"	0.6	7.116	"	"
		30	"	"	"	"	"	"	0.4	4.744	"	"

Table 1 : Beam and Opening Data - General Tests (Continued)

Test	Beam	No.	d	b	t	w	σ_{yf}	σ_{yw}	2h	2a	e
E	W16x40	1E	16.00	7.00	0.503	0.307	34.8	40.0	6.4	12.8	1.0
		2E	"	"	"	"	34.4	40.0	"	"	2.0
		3E	"	"	"	"	34.8	40.2	"	"	1.0
		4E	"	"	"	"	36.1	40.3	"	"	2.0
F	W16x40	1	16.00	7.00	0.503	0.307	34.8	40.0	6.50	12.81	1.0
		2	"	"	"	"	34.4	40.0	6.44	12.75	2.0
		3	"	"	"	"	34.8	40.2	6.38	12.81	1.0
		4	"	"	"	"	36.1	40.3	6.44	12.81	2.0

Beam and Opening Data - Specific Tests

Table 2

Beam No.	e	Experimental M/V	Experimental V_t/V_b	Theoretical M/V *	Theoretical V_t/V_b
1	1.0	40.0	.52	39.2	.48
2	2.0	40.0	.23	40.8	.22
3	1.0	0.0	.41	0.0	.51
4	2.0	0.0	.21	0.0	.25

* Due to the use of incremental shear values in the computer program, an exact M/V value of 40.0 was not obtained for comparison purposes. However, the indicated values are close enough to afford a reasonable comparison.

Shear Force Distribution Results

Table 3

THIS BOOK CONTAINS NUMEROUS PAGES WITH DIAGRAMS THAT ARE CROOKED COMPARED TO THE REST OF THE INFORMATION ON THE PAGE.

THIS IS AS RECEIVED FROM CUSTOMER.

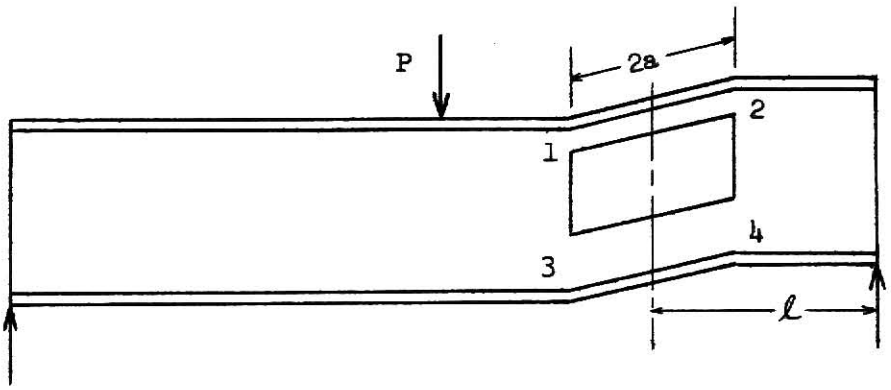

Assumed Mechanism

(a)

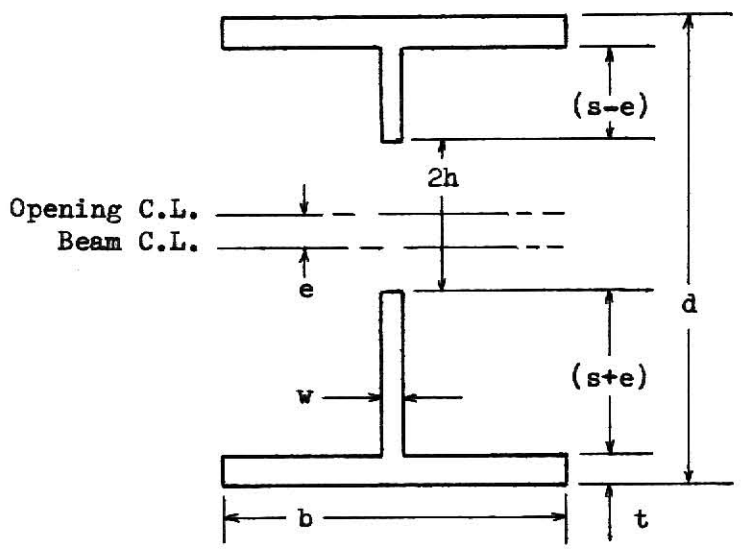

Cross Section Through Opening

(b)

Fig. 1

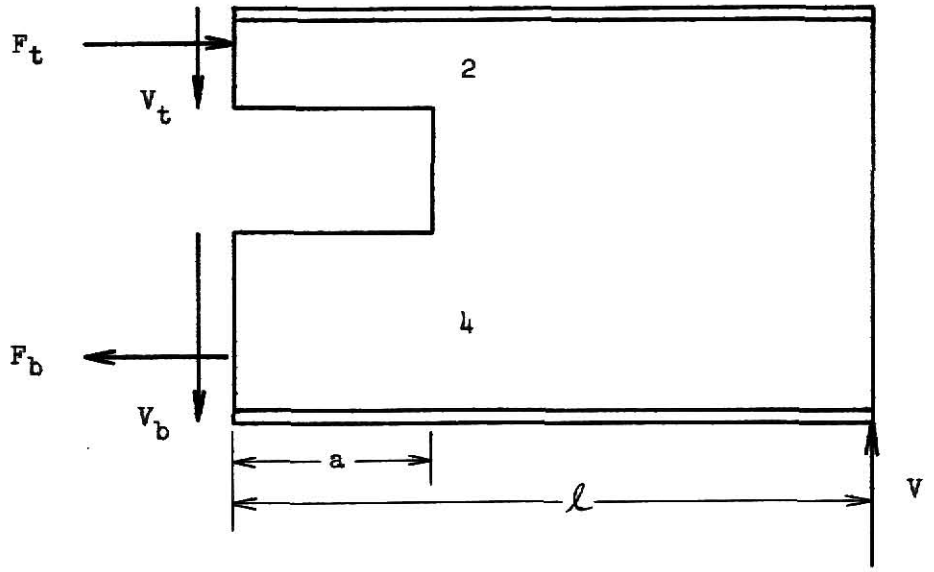

Equilibrium Diagram

Fig. 2

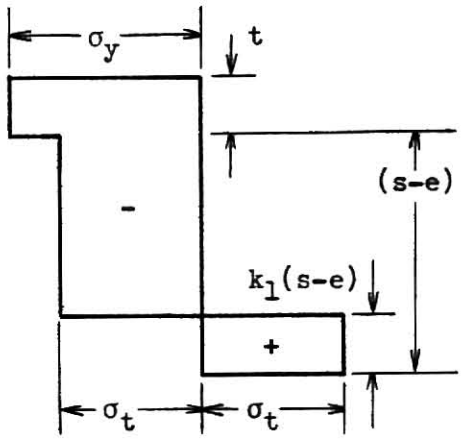

Stress Reversal in Web

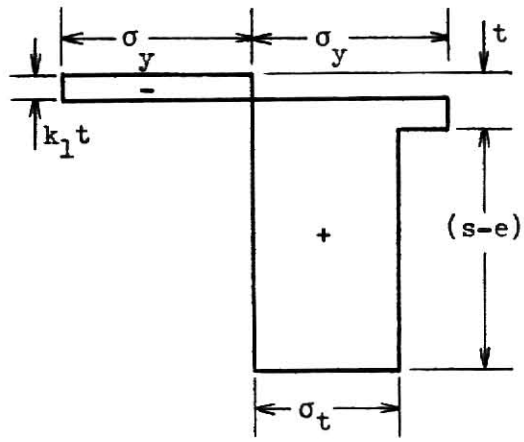

Stress Reversal in Flange

Section 1

(a)

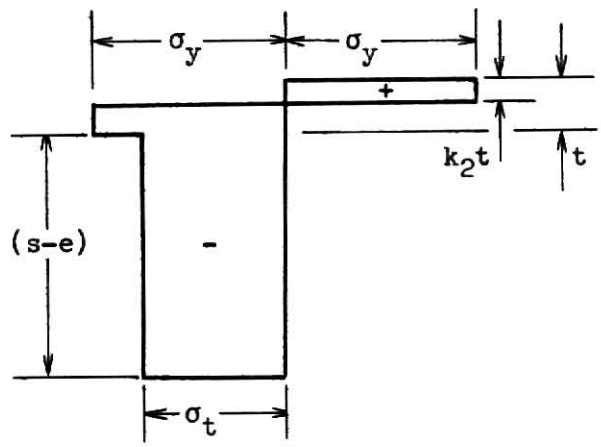

Stress Reversal in Flange Only

Section 2

(b)

Stress Distribution Diagrams

Fig. 3

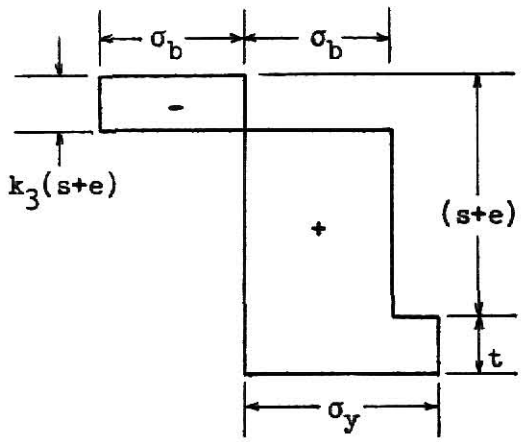

Stress Reversal in Web

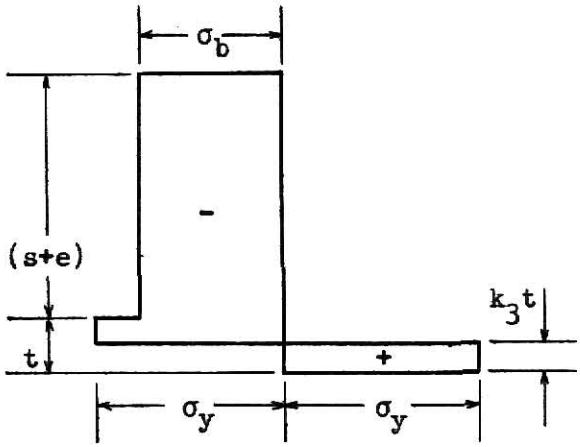

Stress Reversal in Flange

Section 3

(c)

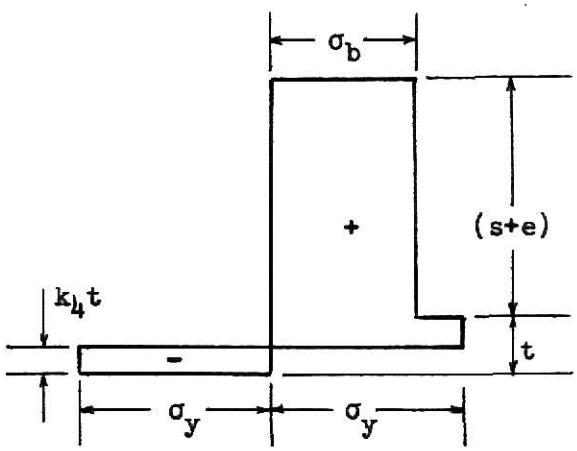

Stress Reversal in Flange Only

Section 4

(d)

Stress Distribution Diagrams

Fig. 3 (continued)

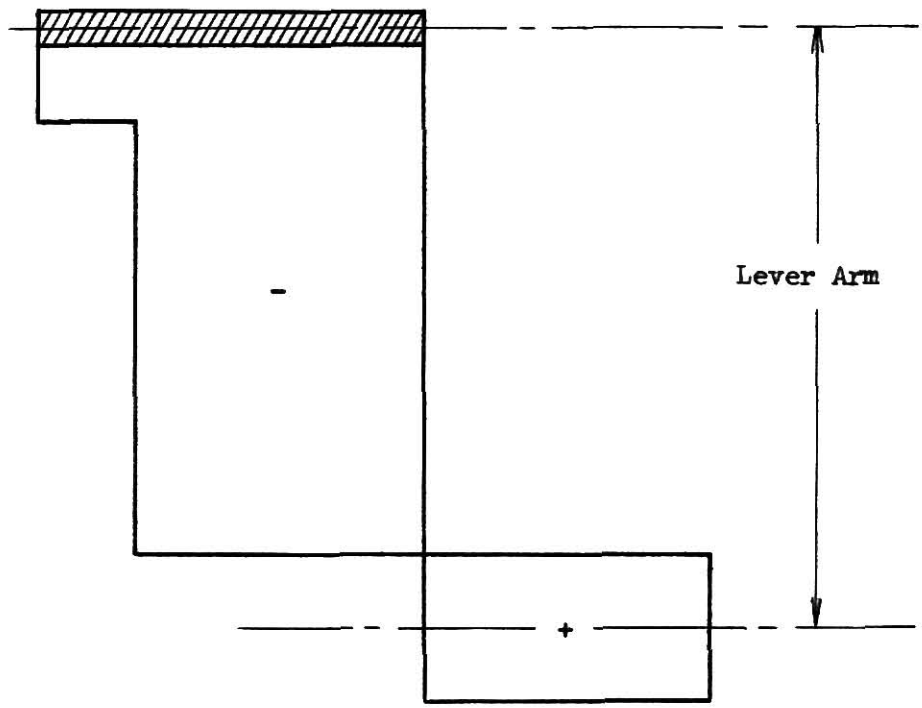

Assumption d: The balancing portion of the negative distribution will be at the opposite end from the positive distribution to maximize the lever arm between the two.

Fig. 4

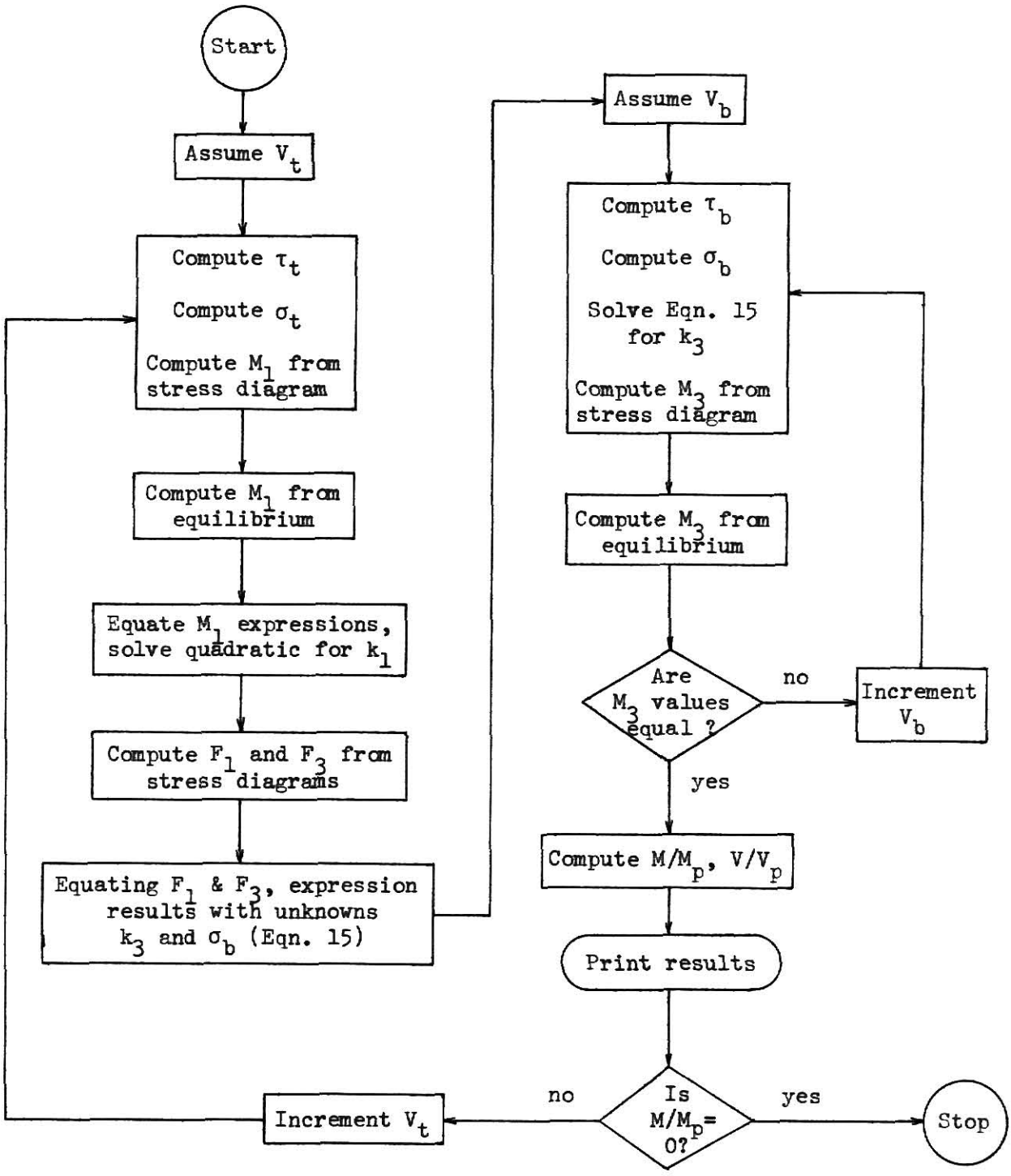

Flow Diagram

Fig. 5

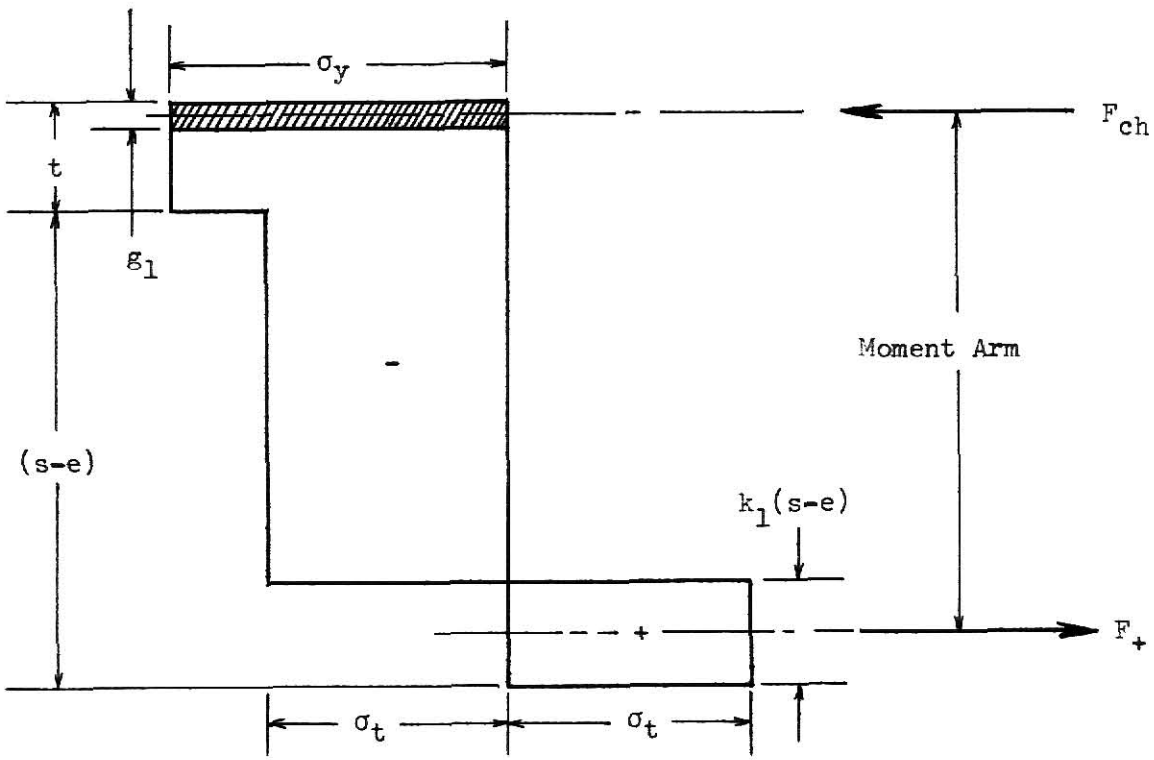

Stress Reversal in Web

Section 1

Internal Resisting Secondary Moment

Fig. 6

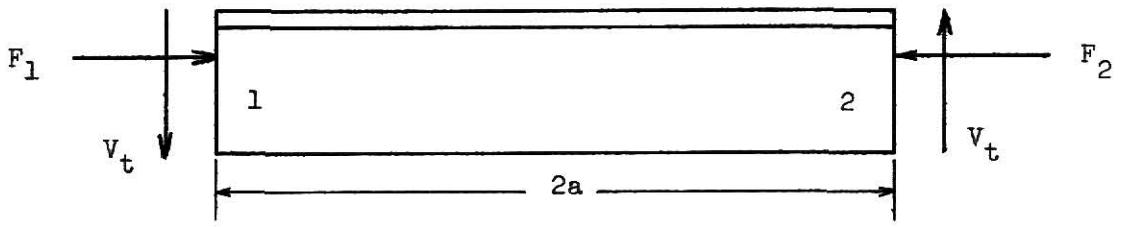

Forces Acting on Top Tee Section

(a)

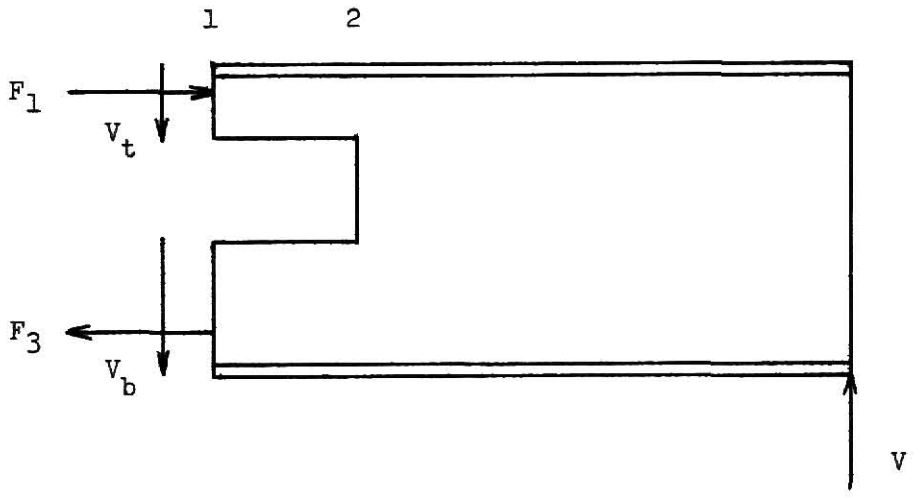

Forces Acting on Section 1 - 3

(b)

Equilibrium Diagrams

Fig. 7

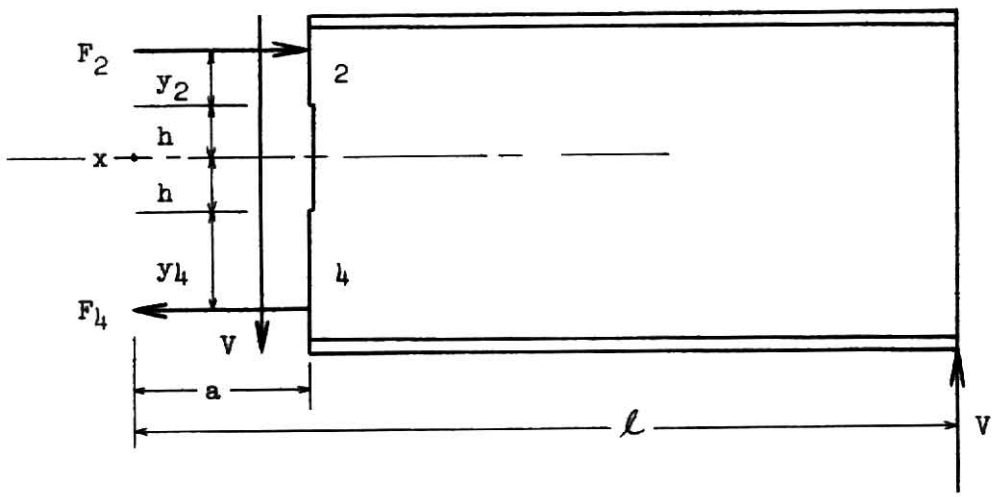

Equilibrium Diagram - Section 2 - 4

Fig. 8

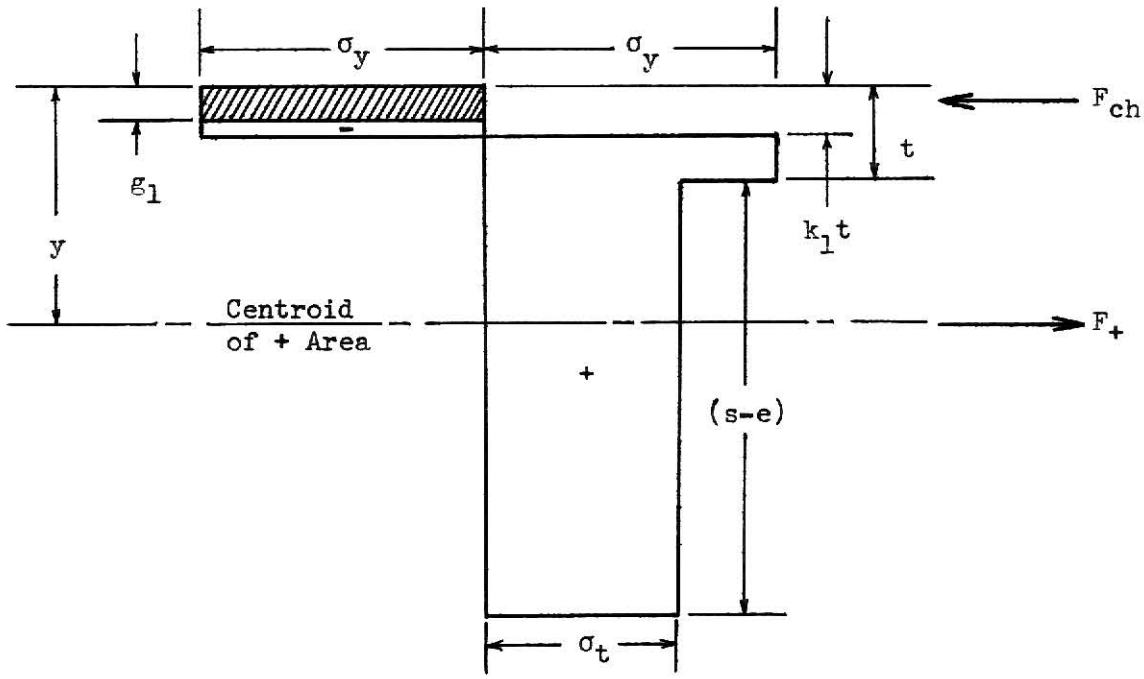

Stress Reversal in Flange

Section 1

Internal Resisting Secondary Moment

Fig. 9

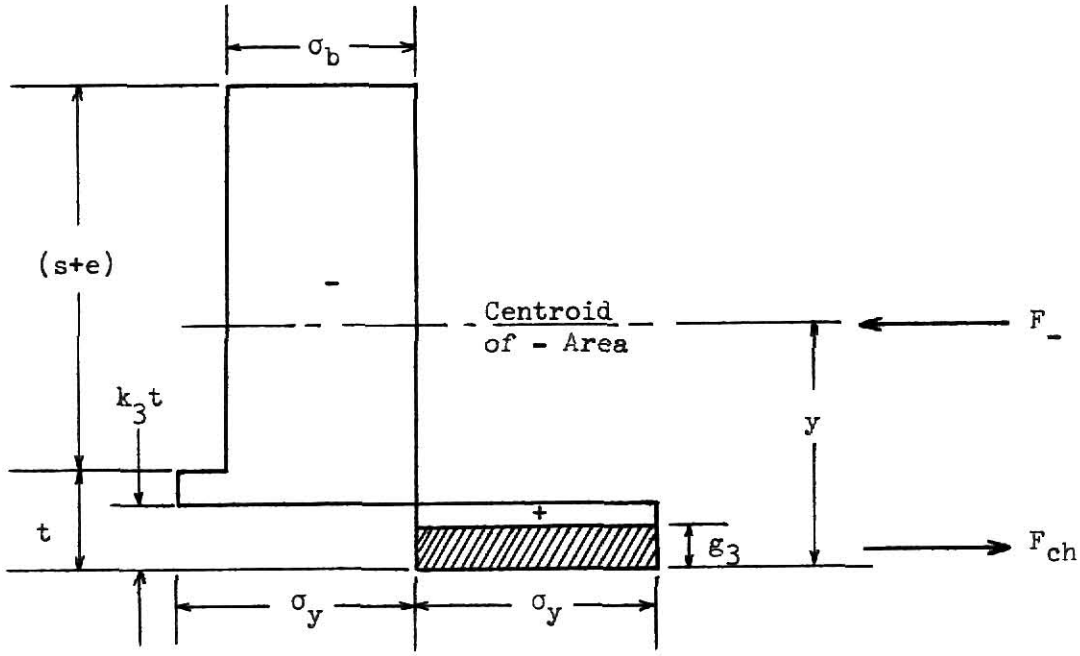

Stress Reversal in Flange

Section 3

Internal Resisting Secondary Moment

Fig. 10

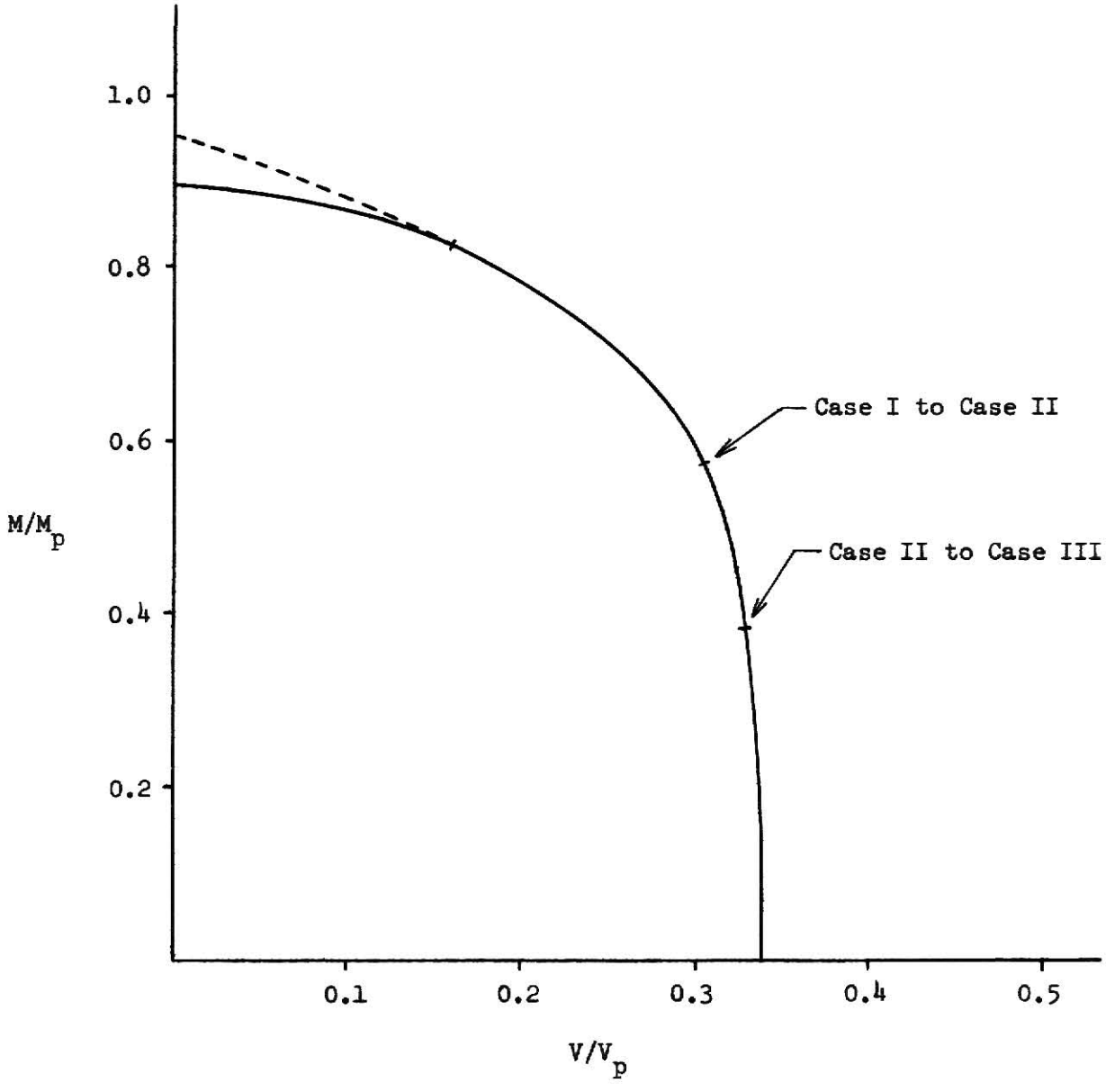

Interaction Curve

Fig. 11

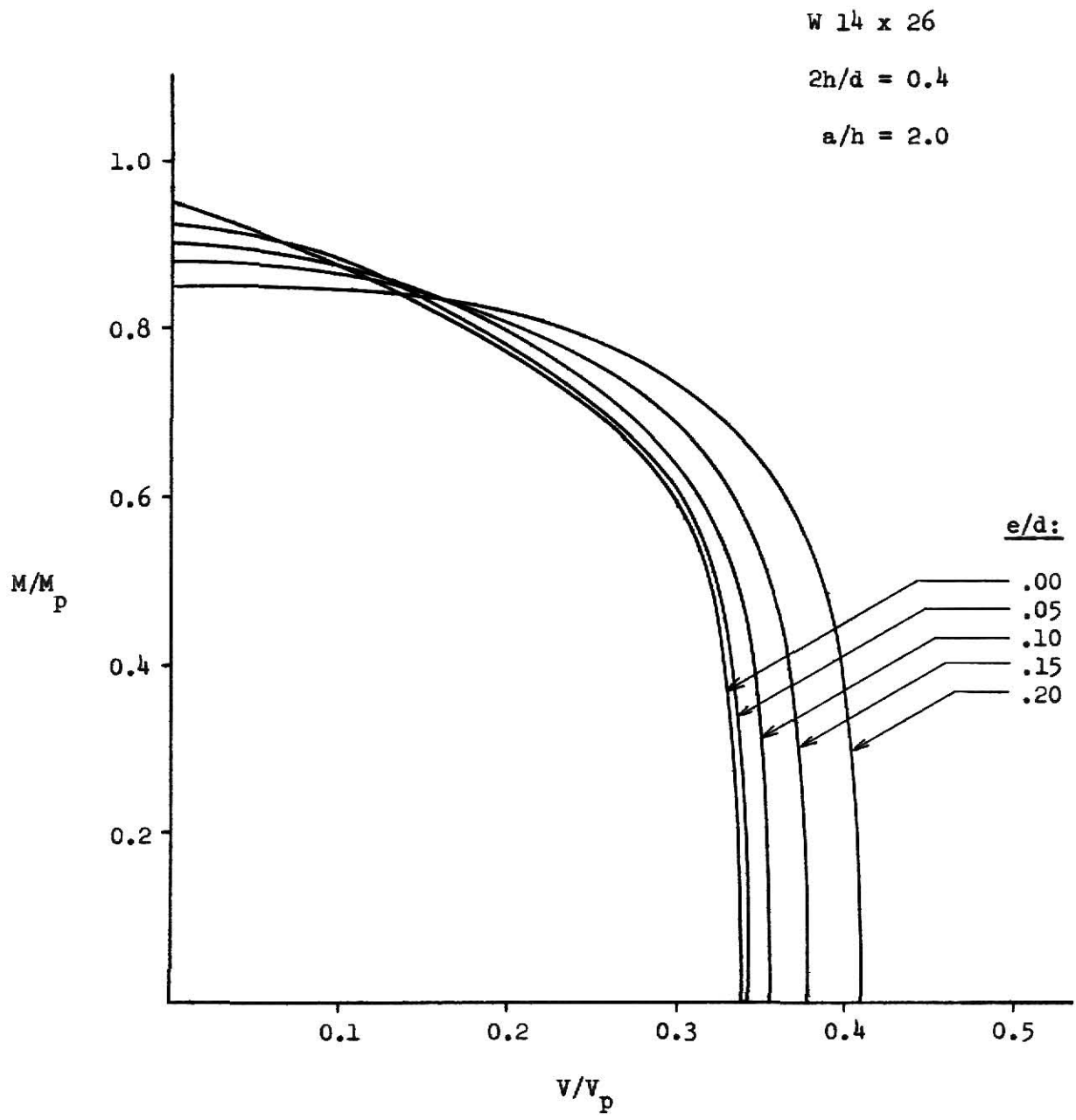

Interaction Curve - Test Beam A1

Fig. 12

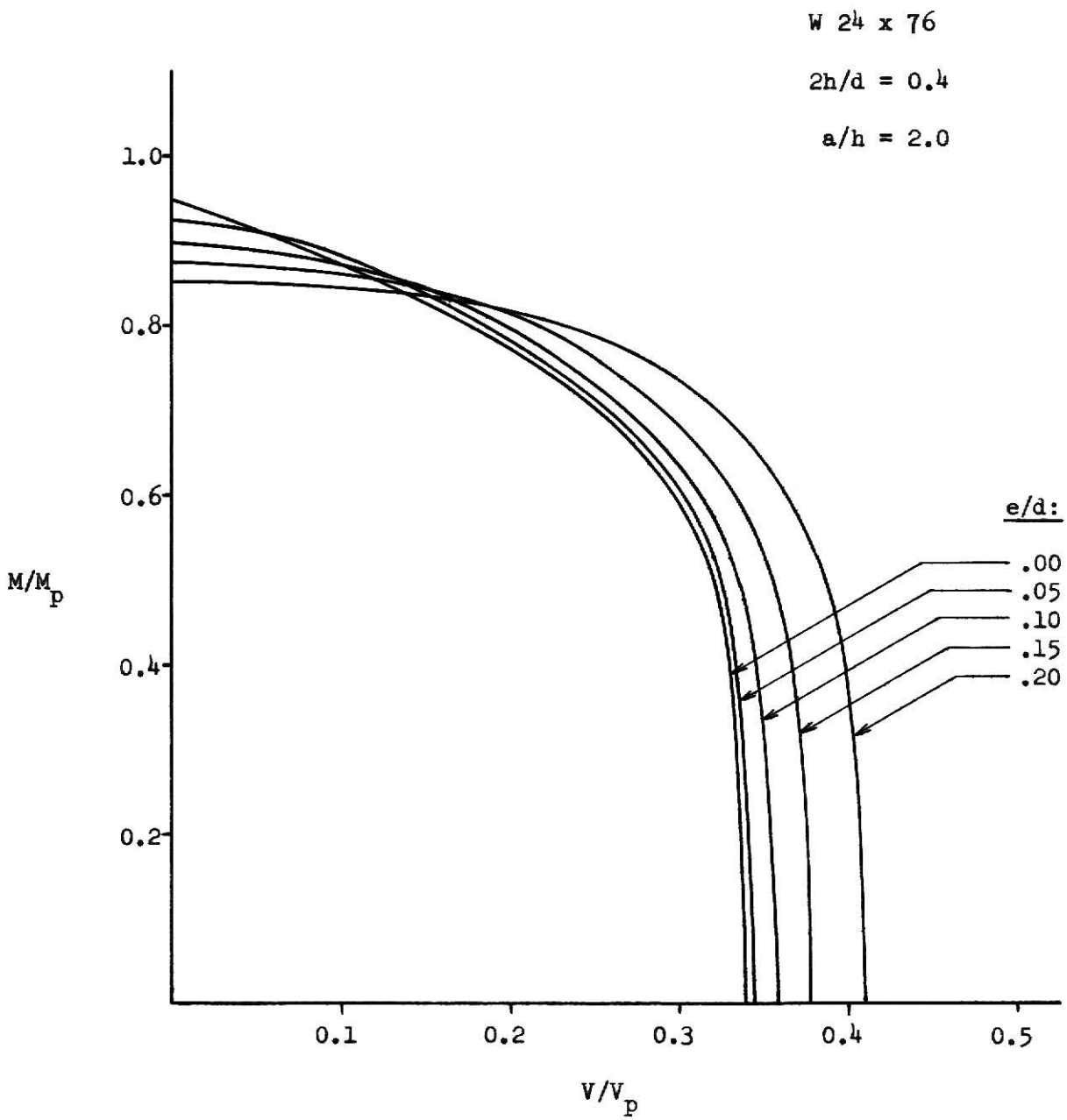

Interaction Curve - Test Beam A2

Fig. 13

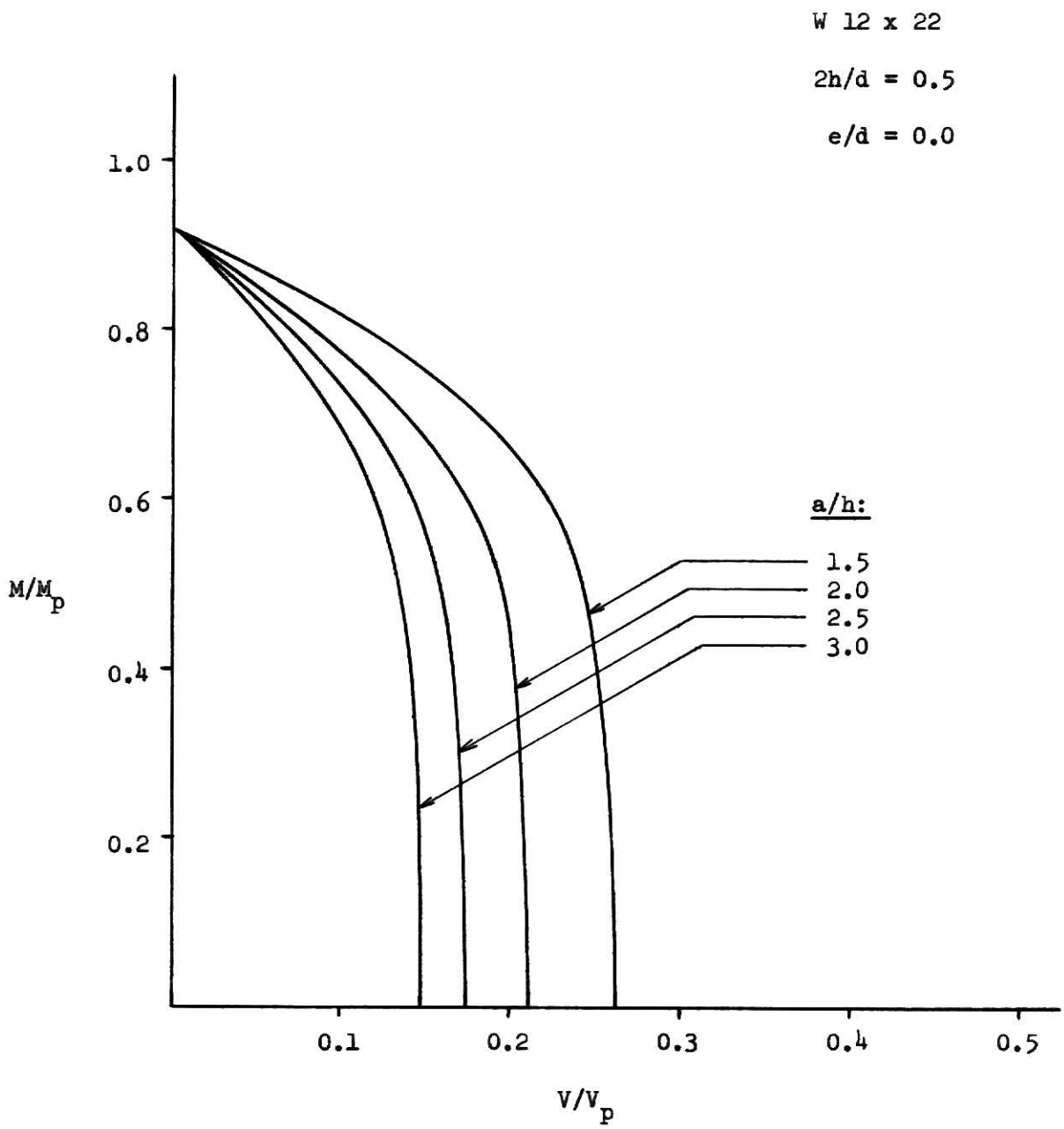

Interaction Curve - Test Beam B1

Fig. 14

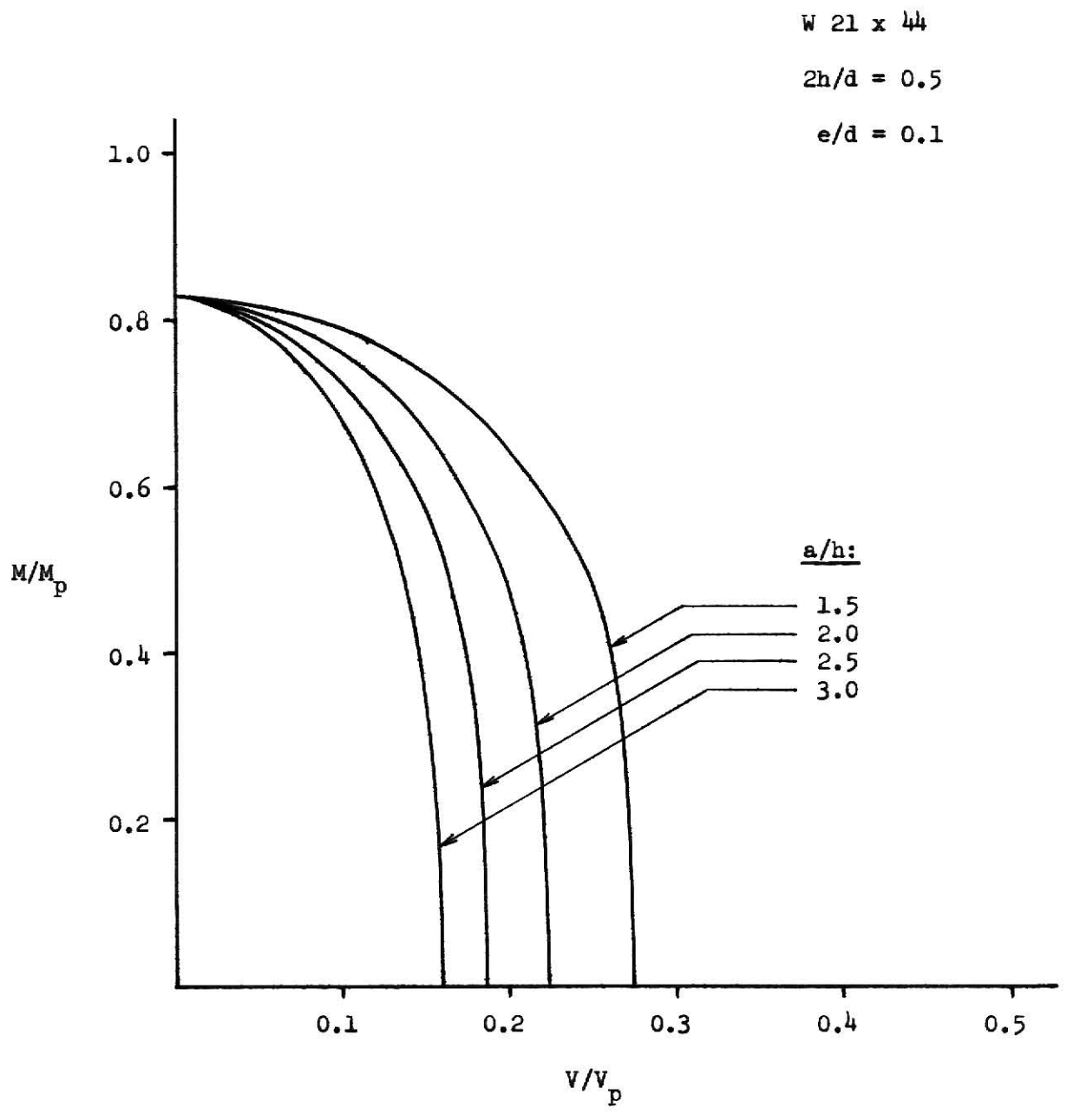

Interaction Curve - Test Beam B2

Fig. 15

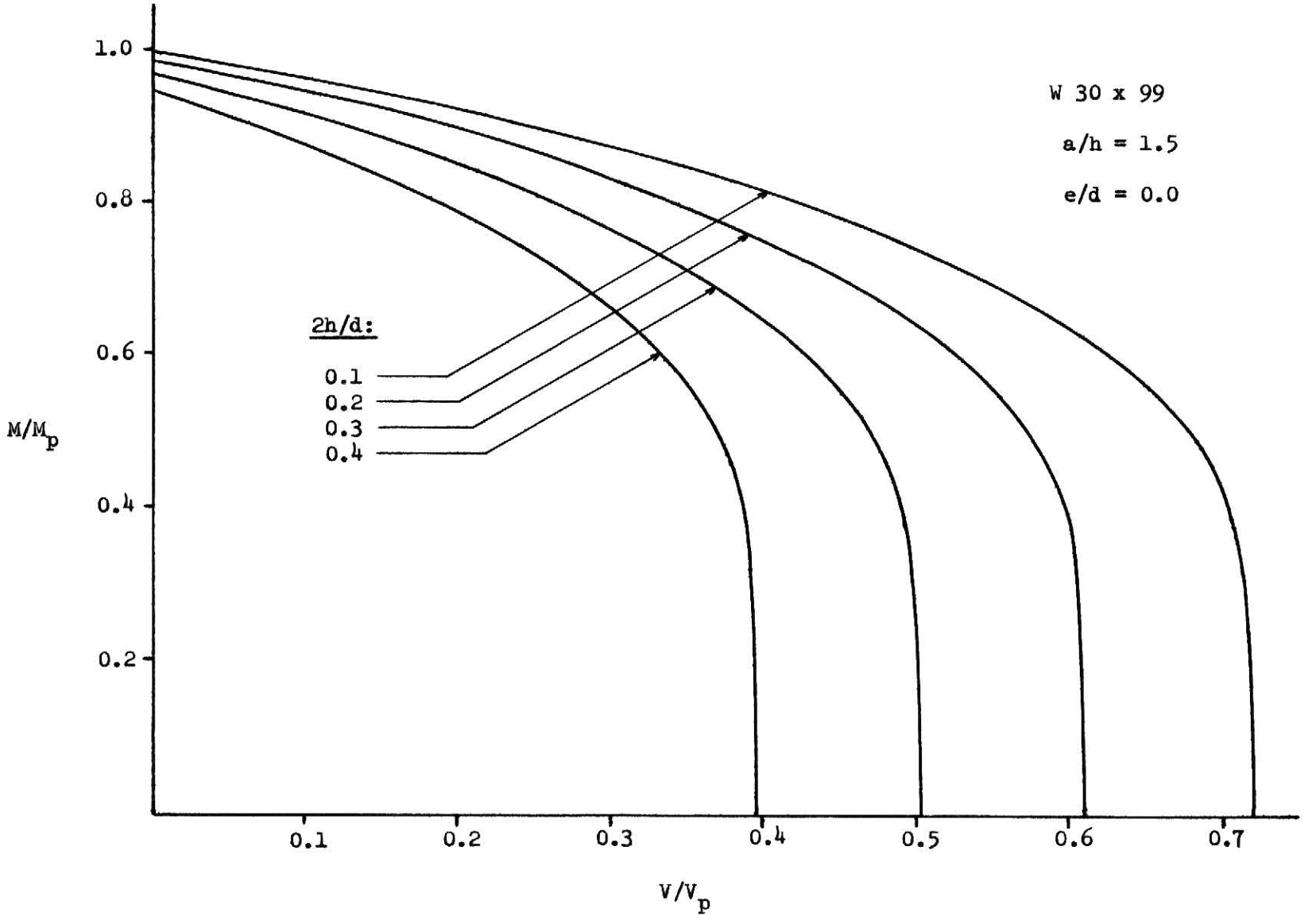

Interaction Curve - Test Beam C1

Fig. 16

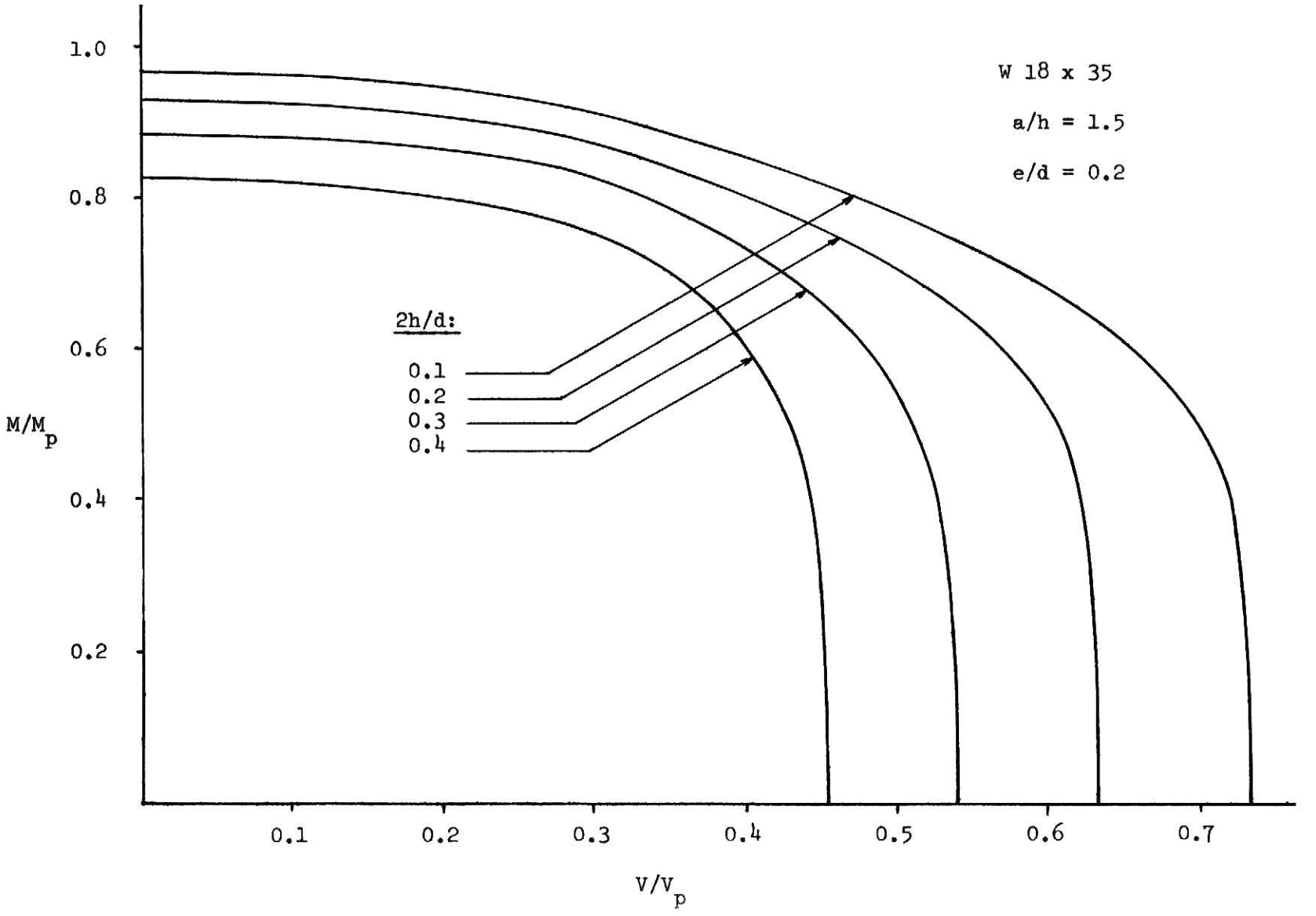

Interaction Curve - Test Beam C2

Fig. 17

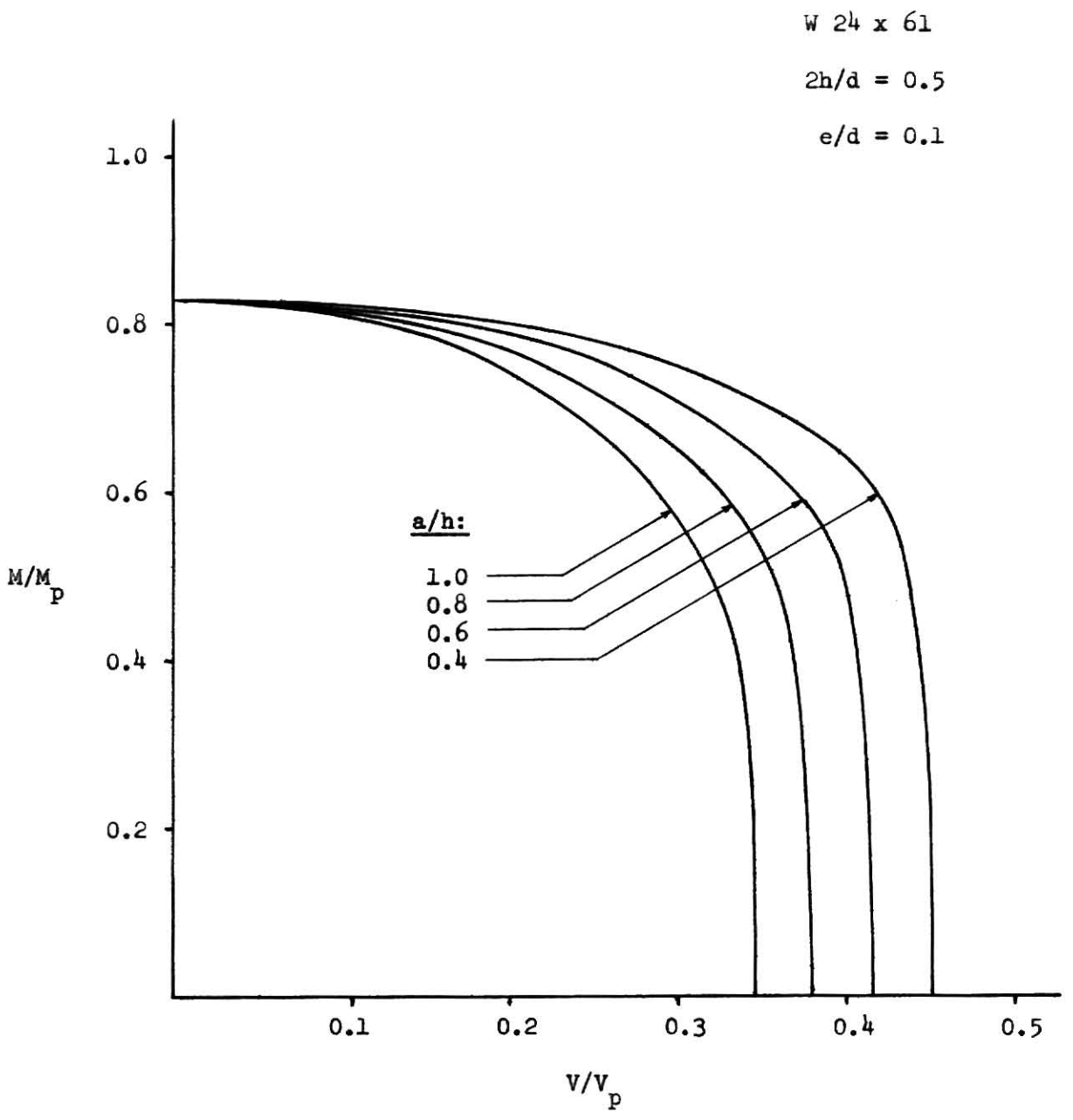

Interaction Curve - Test Beam D

Fig. 18

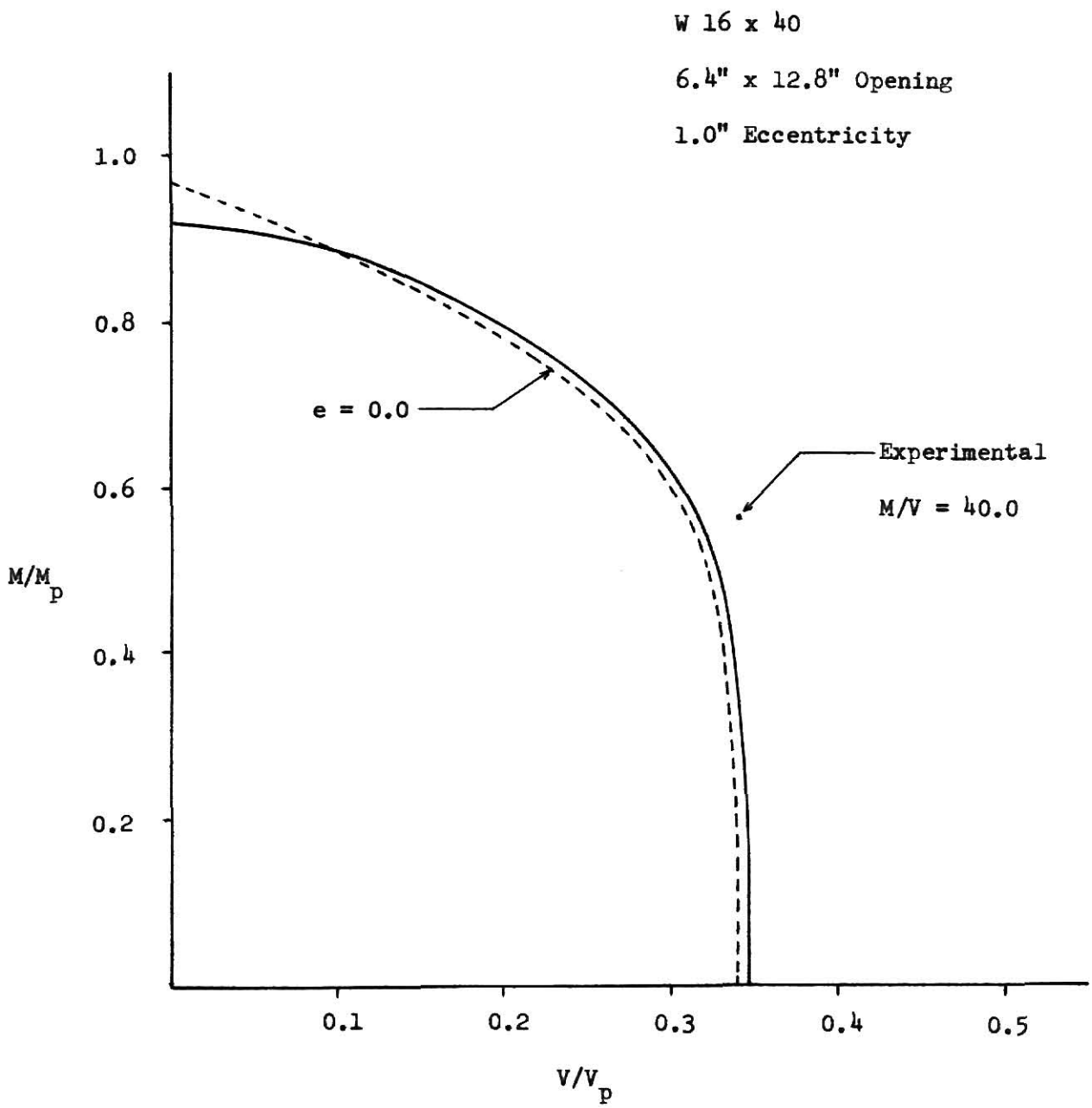

Interaction Curve - Test Beam 1E

Fig. 19

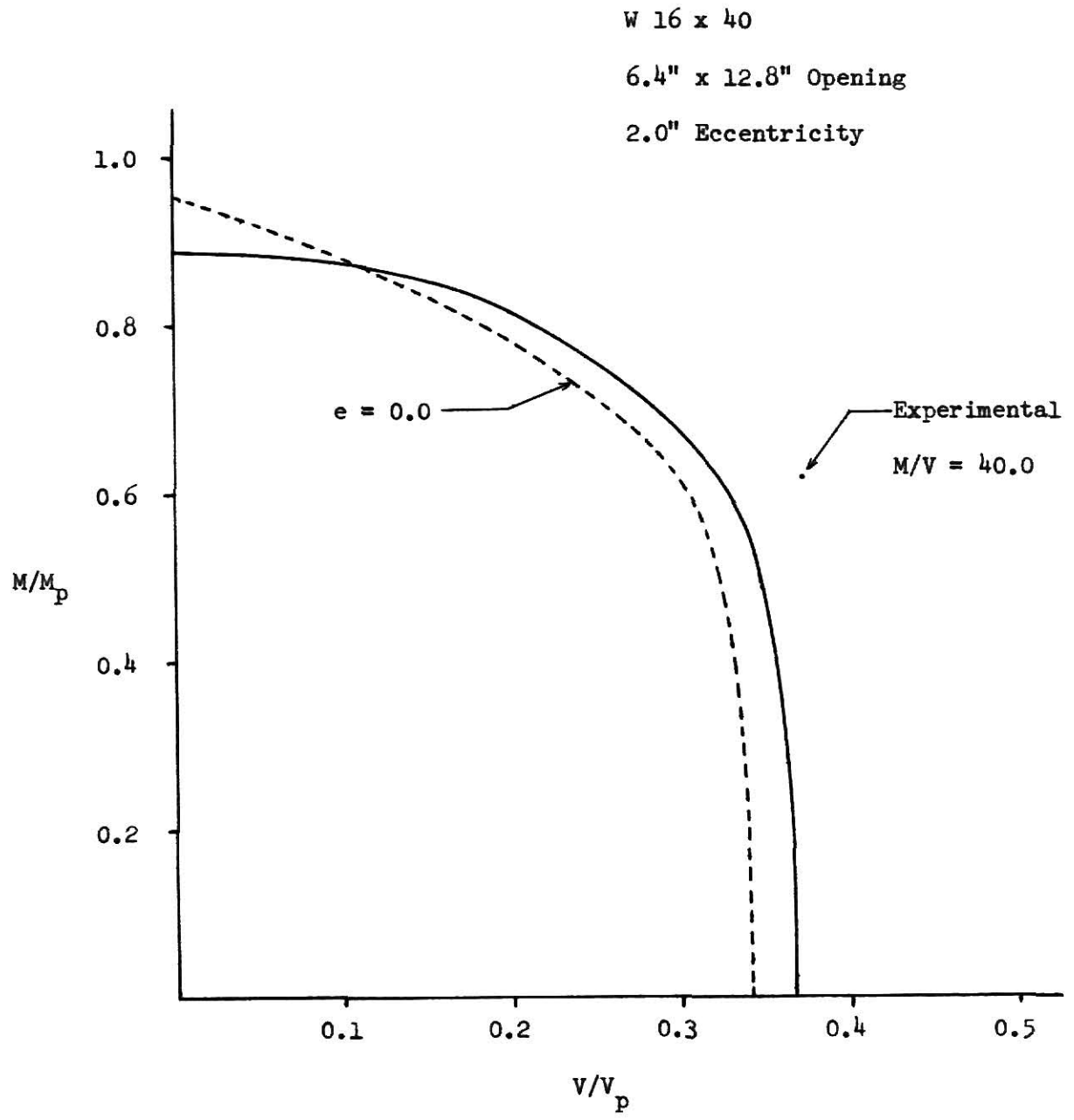

Interaction Curve - Test Beam 2E

Fig. 20

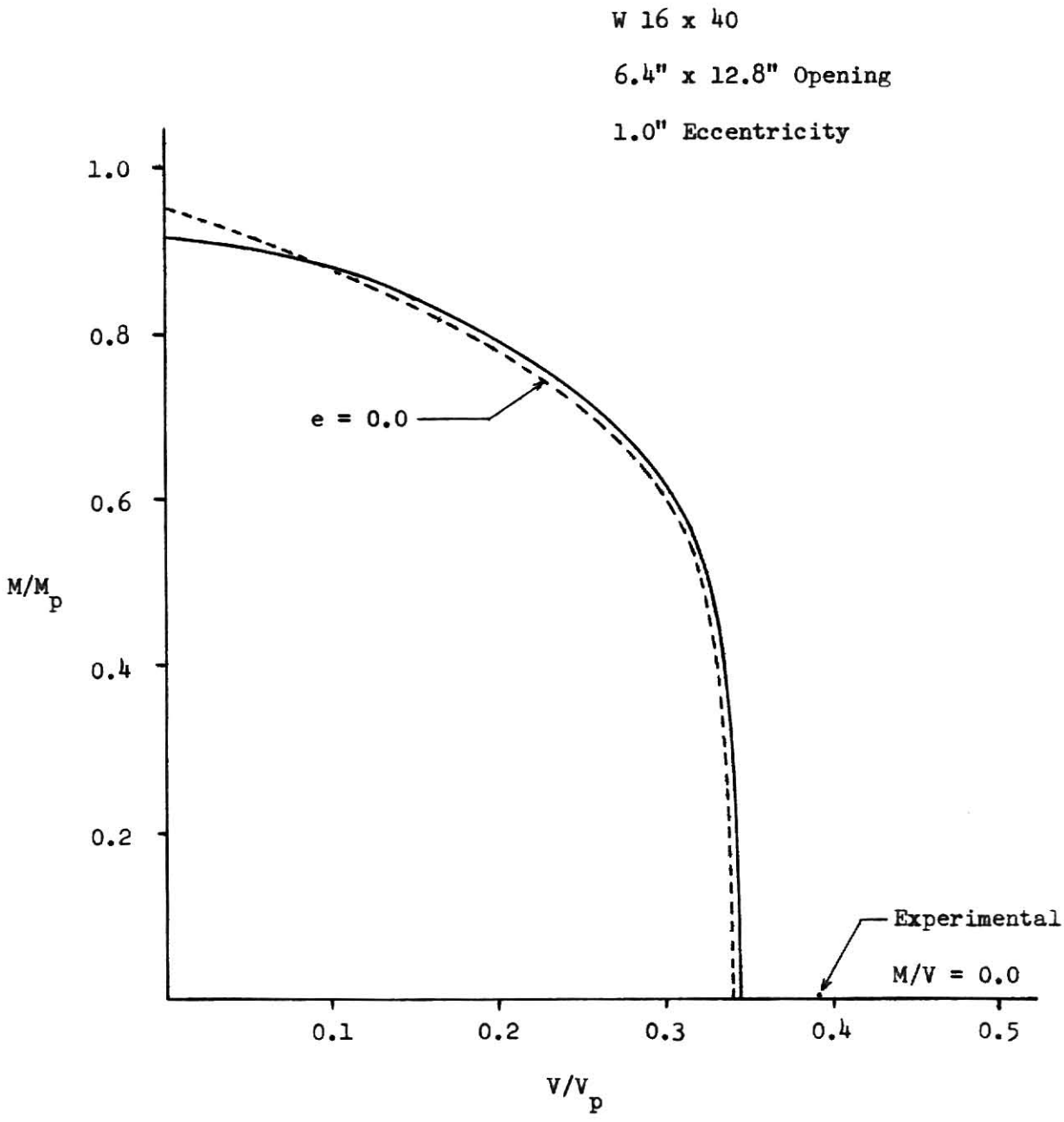

Interaction Curve - Test Beam 3E

Fig. 21

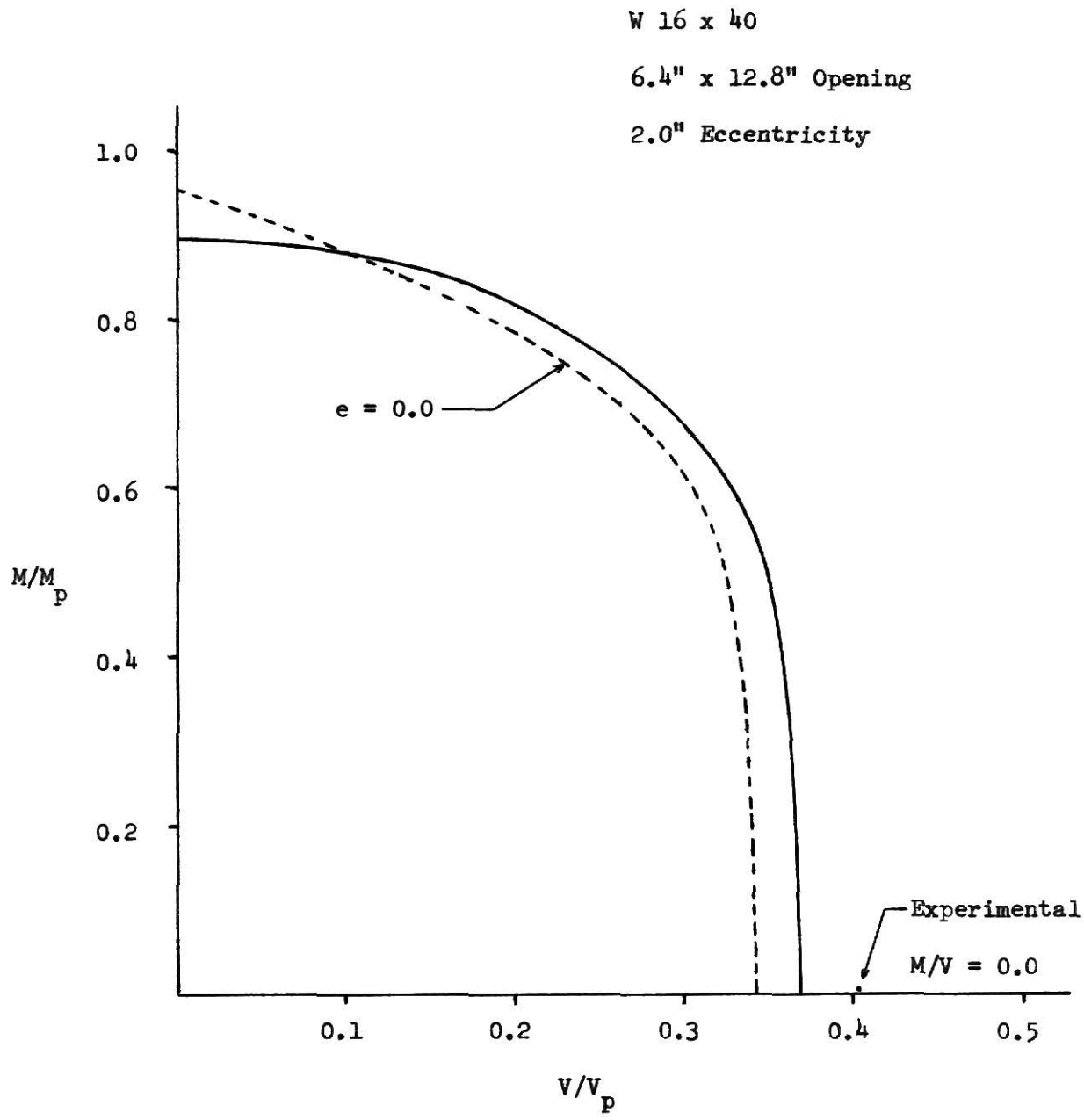

Interaction Curve - Test Beam 4E

Fig. 22

APPENDIX A

Nomenclature

a	Half length of opening
A_f	Flange area (b x t)
A_w	Total web area (s x w)
b	Flange width
d	Depth of Beam
e	Opening eccentricity
F_1	Total normal force, section one
F_2	Total normal force, section two
F_3	Total normal force, section three
F_4	Total normal force, section four
F_-	Force due to negative stress block
F_+	Force due to positive stress block
F_{ch}	Force due to crosshatched portion of stress block
g_1	Depth of resisting stress block, section one
g_3	Depth of resisting stress block, section three
h	Half depth of opening
k_1	Stress reversal coefficient, section one
k_2	Stress reversal coefficient, section two
k_3	Stress reversal coefficient, section three
k_4	Stress reversal coefficient, section four
ℓ	Horizontal distance from opening centerline to closest support
M_1	Secondary moment, section one
M_2	Secondary moment, section two

M_3 Secondary moment, section three

M_4 Secondary moment, section four

M_p Plastic moment capacity, uncut section

M_x Moments about point x

M_{pi} Plastic moment capacity, zero shear

P Concentrated load

s Half of total web depth at opening (d/2 - t - h)

t Flange thickness

V Total shear force ($V_t + V_b$)

V_b Shear force, botton tee section

V_ℓ Shear limit

V_p Plastic shear capacity, uncut section

V_t Shear force, top tee section

w Web thickness

y Depth from edge of flange to centroid of positive and negative stress blocks for sections one and three respectively

y_2 Distance from opening edge to total normal force, section two

y_4 Distance from opening edge to total normal force, section four

σ_b Normal stress, bottom tee section

σ_n Normal stress

σ_t Normal stress, top tee section

σ_y Yield stress

σ_{yf} Flange yield stress

σ_{yw} Web yield stress

τ Shear stress

τ_b Shear stress, bottom tee section

τ_t Shear stress, top tee section

APPENDIX B

Computer Program

A computer program was developed to compute the interaction curve relating moment and shear capacities for wide flange beams containing eccentric rectangular unreinforced web openings. The program was written in Fortran IV and is shown on the following pages. Three data cards are necessary for each sample beam and one card is necessary to indicate how many beams will be analyzed. A sample data table follows:

Card	Description	Items
1	Number of beams to be analyzed	No. beams
2	Beam 1, beam dimensions	d, b, t, w
3	Beam 1, opening dimensions	2h, 2a, e
4	Beam 1, flange & web yield stresses	σ_{yf}, σ_{yw}
5	Beam 2, beam dimensions	d, b, t, w
	Etc.	

```
 5 FORMAT (1I2)
10 FORMAT (4F10.4)
20 FORMAT (3F10.4)
30 FORMAT (2F10.4)
35 FORMAT (///)
40 FORMAT(40H INTERACTION BETWEEN MOMENT AND SHEAR -
  1 8HSPECIMEN1I3//)
50 FORMAT (39H     BEAM       FLANGE      FLANGE      WEB )
51 FORMAT (41H     DEPTH      WIDTH       THICK.     THICK. /)
60 FORMAT (/29H     HOLE       HOLE        ECC.   )
61 FORMAT (19H     DEPTH     LENGTH /)
70 FORMAT (/18H     FLANGE      WEB)
71 FORMAT (19H     YIELD      YIELD)
72 FORMAT (20H     STRESS     STRESS/)
80 FORMAT (/7H CASE I /)
81 FORMAT (/8H CASE II/)
82 FORMAT (/9H CASE III /)
85 FORMAT (//61H                PLASTIC              PLASTIC
  1  SHEAR       )
86 FORMAT (65H                  SHEAR                MOMENT
  1LIMIT       /)
88 FORMAT (/117H       M/MP       V/VP       M          V          VT
  1    VB         SIG T      SIG B        K1         K2         K3
  12HK4)
 1 FORMAT (3F20.4//)
 2 FORMAT (2F10.4,1F10.1,3F10.4,2F10.3,4F10.4)
   READ 5,NB
   N=1
 8 PRINT 40,N
   PRINT 50
   PRINT 51
   READ 10,D,B,T,W
   PRINT 10,D,B,T,W
   PRINT 60
   PRINT 61
   READ 20,H,A,E
   PRINT 20,H,A,E
   H=H/2.0
   A=A/2.0
   READ 30,SIGY,SIGYW
   S=D/2.0-T-H
   PV=W*(D-2.0*T)*SIGYW/3.0**0.5
   PM=B*T*SIGY *(D-T)+W*(D-2.0*T)**2*SIGYW/4.0
   VPVM=(D-2.0*T-2.0*H)/(D-2.0*T)
   PRINT 70
   PRINT 71
   PRINT 72
   PRINT 30,SIGY,SIGYW
   PRINT 85
   PRINT 86
   PRINT 1,PV,PM,VPVM
```

```
      PRINT 88
      PRINT 80
      AW=S*W
      AF=B*T
      IF (E)  12,14,12
   12 ZM=AF*SIGY*(D-T)+SIGYW*W*(S*D-2.0*S*T-S**2-E*D+2.0*E*T+
     12.0*E*S)
      GO TO 16
   14 ZM=2.0*SIGY*AF*(S+H+T/2.0)+2.0*AW*SIGYW*(S/2.0+H)
   16 Z=ZM/PM
      V=0.0
      PRINT 2,Z,V,ZM,V,V,V,SIGYW,SIGYW,V,V,V,V
      VINCR=0.0
      J=1
      K=1
      L=1
      MM=1
      IF (E)  96,95,96
   95 VT=0.0
      VINCR=PV/100.0
      L=L-2
      GO TO 99
   96 VT=0.00005
      GO TO 99
   97 VT=VI
   99 VT=VT+VINCR
      TT=VT/(W*(S-E))
      XX=SIGYW**2-3.0*TT**2
      IF (XX)  503,100,100
  100 SIGT=XX**0.5
      A1=((S-E)**2*SIGT*W/2.0)*(SIGT*W/(SIGY*B)+1.0)
      A2=-SIGT*W*(S-E)*(S-E+T)
      A3=VT*A
      A4=A2**2-4.0*A1*A3
      IF (A4)  101,110,110
  110 C1=(-A2+A4**0.5)/(2.0*A1)
      C1A=(-A2-A4**0.5)/(2.0*A1)
      IF (C1)  120,112,112
  112 IF (C1-1.0)  126,126,120
  120 IF (C1A)  101,122,122
  122 IF (C1A-1.0)  124,124,101
  101 C1=1.0
      VT=VT-VINCR
  102 TT=VT/(W*(S-E))
      XX=SIGYW**2-3.0*TT**2
      IF (XX)  503,103,103
  103 SIGT=XX**0.5
      ZM1=SIGT*W*(S-E)*(S-E+T)-((S-E)**2*SIGT*W/2.0)*(SIGT*W/
     1(SIGY*B)+1.0)
      ZM1A=VT*A
      IF (MM-1)  104,115,104
```

```
 104 IF (MM-2)  105,116,105
 105 IF (MM-3)  106,117,106
 106 IF (MM-4)  107,118,107
 107 IF (MM-5)  1199,119,1199
 115 IF (ZM1-ZM1A)  1160,1199,1150
1150 VT=VT+1.0
     GO TO 102
1160 VT=VT-0.1
     MM=2
     GO TO 102
 116 IF (ZM1-ZM1A)  1160,1199,1170
1170 VT=VT+0.01
     MM=3
     GO TO 102
 117 IF (ZM1-ZM1A)  1180,1199,1170
1180 VT=VT-0.001
     MM=4
     GO TO 102
 118 IF (ZM1-ZM1A)  1180,1199,1190
1190 VT=VT+0.0001
     MM=5
     GO TO 102
 119 IF (ZM1-ZM1A)  1199,1199,1190
1199 MM=0
     GO TO 126
 124 C1=C1A
 126 F=AF*SIGY+SIGT*W*(S-E)*(1.0-2.0*C1)
 127 C2=0.5-((F-(S-E)*W*SIGT)/(2.0*AF*SIGY))
     IF (C2)  900,128,128
 128 IF (C2-1.0)  130,130,900
 130 VB=VT
 133 M=1
     Q1=W*(S+E)
     Q2=SIGYW**2
     Q3=(F-AF*SIGY)/(2.0*Q1)
     Q4=S+E+T
     Q5=(S+E)/2.0
     Q6=W/(B*SIGY)
     Q7=2.0*AF*SIGY
     Q8=AF*T*SIGY
     Q9=(S+E)**2*W/2.0
 132 TB=VB/Q1
     YY=Q2-3.0*TB**2
     IF (YY)  505,135,135
 135 SIGB=YY**0.5
     IF (K)  310,310,136
 136 C3=0.5-Q3/SIGB
     IF (L)  137,159,137
 159 B1=((S+E)**2*W*SIGB/2.0)*(1.0+W*SIGB/(B*SIGY))
     B2=-(S+E)*W*SIGB*(S+E+T)
     B3=VB*A
```

```
      B4=B2**2-4.0*B1*B3
      IF (B4)  200,1591,1591
1591  C3=(-B2+B4**0.5)/(2.0*B1)
      C3A=(-B2-B4**0.5)/(2.0*B1)
      IF (C3)  1595,1592,1592
1592  IF (C3-1.0)  1593,1593,1595
1595  IF (C3A)  200,1594,1594
1594  IF (C3A-1.0)  1596,1596,200
1596  C3=C3A
1593  C4=C3*SIGB*W*(S+E)/(AF*SIGY)
      IF (C4)  900,1111,1111
1111  IF (C4-1.0)  167,167,900
 137  ZM3=C3*SIGB*Q1*(Q4-(C3*Q5*(SIGB*Q6+1.0)))
      Z=VB*A
      IF (M-1)  141,145,141
 141  IF (M-2)  142,148,142
 142  IF (M-3)  143,150,143
 143  IF (M-4)  144,152,144
 144  IF (M-5)  200,154,200
 145  IF (Z-ZM3)  146,160,147
 146  VB=VB+1.0
      GO TO 132
 147  VB=VB-0.1
      M=2
      GO TO 132
 148  IF (Z-ZM3)  149,160,147
 149  VB=VB+0.01
      M=3
      GO TO 132
 150  IF (Z-ZM3)  149,160,151
 151  VB=VB-0.001
      M=4
      GO TO 132
 152  IF (Z-ZM3)  153,160,151
 153  VB=VB+0.0001
      M=5
      GO TO 132
 154  IF (Z-ZM3)  153,160,160
 160  C4=C3*SIGB*W*(S+E)/(AF*SIGY)
      IF (C4)  900,161,161
 161  IF (C4-1.0)  162,162,900
 162  IF (C3)  300,163,163
 163  IF (C3-1.0)  164,164,300
 164  IF (L)  167,167,165
 165  VB5=VB
      VBI=VB/2.9
      VB=0.0
      L=L-1
 168  VB=VB+VBI
      IF (VB5-VB)  169,132,132
 169  L=L-1
```

```
      VINCR=PV/100.0
      GO TO 99
  167 V=VT+VB
      FY2A=(S-E)*(1.0-2.0*C2)+T*0.5*(2.0*C2**2-4.0*C2+1.0)
      FY2=0.5*W*SIGT*(S-E)**2+AF*SIGY*FY2A
      FY4A=(S+E)*(1.0-2.0*C4)+0.5*T*(2.0*C4**2-4.0*C4+1.0)
      FY4=0.5*W*SIGB*(S+E)**2+AF*SIGY*FY4A
      ZM=FY2+FY4+F*2.0*H+V*A
      ZMP=ZM/PM
      VVP=V/PV
      IF (K)  302,302,166
  166 IF (J)  202,202,171
  171 PRINT 2,ZMP,VVP,ZM,V,VT,VB,SIGT,SIGB,C1,C2,C3,C4
      IF (L)  174,168,168
  174 IF (MM)  199,199,99
  199 VT=VT+PV/1000.0
  200 IF (E)  201,300,201
  201 I=1
      J=J-1
      VINCR=PV/1000.0
      GO TO 208
  202 IF (I)  205,205,204
  204 PRINT 81
      I=I-1
  205 PRINT 2,ZMP,VVP,ZM,V,VT,VB,SIGT,SIGB,C1,C2,C3,C4
      GO TO 203
 2055 VT=VI
  203 VT=VT+VINCR
      TT=VT/(W*(S-E))
      XX=SIGYW**2-3.0*TT**2
      IF (XX)  500,206,206
  206 SIGT=XX**0.5
  208 B1=AF*T*SIGY
      B2=-AF*SIGY*T-T*(S-E)*W*SIGT
      B3=-((S-E)**2*W*SIGT/2.0)*(1.0-W*SIGT/(B*SIGY))+VT*A
      B4=B2**2-4.0*B1*B3
      IF (B4)  500,210,210
  210 C1=(-B1-B4**0.5)/(2.0*B1)
      C1A=(-B2+B4**0.5)/(2.0*B1)
      IF (C1)  220,212,212
  212 IF (C1-1.0)  224,224,220
  220 IF (C1A)  500,221,221
  221 IF (C1A-1.0)  223,223,500
  223 C1=C1A
  224 F=AF*SIGY*(2.0*C1-1.0)-(S-E)*W*SIGT
      GO TO 127
  300 I=1
      K=K-1
      VINCR=PV/400.0
      GO TO 208
  302 IF (I)  305,305,304
```

```
304 PRINT 82
    I=I-1
305 IF (ZM)  500,306,306
306 PRINT 2,ZMP,VVP,ZM,V,VT,VB,SIGT,SIGB,C1,C2,C3,C4
    GO TO 203
310 C3=0.5+(F+Q1*SIGB)/Q7
    ZM3=-(C3**2*Q8)+C3*(Q8+T*Q1*SIGB)+(Q9*SIGB)*(1.0-Q6*SIGB)
    Z=VB*A
    IF (M-1)  341,345,341
341 IF (M-2)  342,348,342
342 IF (M-3)  343,350,343
343 IF (M-4)  344,352,344
344 IF (M-5)  900,354,900
345 IF (Z-ZM3)  346,357,347
346 VB=VB+1.0
    GO TO 132
347 VB=VB-0.1
    M=2
    GO TO 132
348 IF (Z-ZM3)  349,357,347
349 VB=VB+0.01
    M=3
    GO TO 132
350 IF (Z-ZM3)  349,357,351
351 VB=VB-0.001
    M=4
    GO TO 132
352 IF (Z-ZM3)  353,357,351
353 VB=VB+0.0001
    M=5
    GO TO 132
354 IF (Z-ZM3)  353,357,357
357 C4=1.0-C3+W*SIGB*(S+E)/(AF*SIGY)
    IF (C4)  900,161,161
500 VT=VT-VINCR
    VINCR=VINCR/10.0
    VIMIN=PV/100000.0
    IF (VINCR-VIMIN)  900,203,203
503 VI=VT-VINCR
    VINCR=VINCR/10.0
    VIMIN=PV/1000000.0
    IF (VINCR-VIMIN)  900,97,97
505 IF (K)  500,500,506
506 VI=VT-VINCR
    VINCR=VINCR/10.0
    VIMIN=PV/1000000.0
    IF (VINCR-VIMIN)  900,507,507
507 IF (J)  2055,2055,97
900 IF (N-NB)  901,902,902
901 N=N+1
    PRINT 35
```

```
      GO TO 8
902   STOP
      END
```

ILLEGIBLE DOCUMENT

THE FOLLOWING DOCUMENT(S) IS OF POOR LEGIBILITY IN THE ORIGINAL

THIS IS THE BEST COPY AVAILABLE

INTERACTION BETWEEN MOMENT AND SHEAR - SPECIMEN 1

BEAM DEPTH	FLANGE WIDTH	FLANGE THICK.	WEB THICK.
20.6600	6.5000	0.4510	0.3480

HOLE DEPTH	HOLE LENGTH	ECC.
10.3300	25.8250	2.0660

FLANGE YIELD STRESS	WEB YIELD STRESS
36.0000	36.0000

PLASTIC SHEAR	PLASTIC MOMENT	SHEAR LIMIT
142.9105	3355.4000	0.4772

M/MP	V/VP	M	V	VT	VB	SIG T	SIG B	K1	K2	K3	K4
CASE I											
0.8207	0.0000	2753.8	0.0000	0.0000	0.0000	36.000	36.000	0.0000	0.0000	0.0000	0.0000
0.8194	0.0234	2749.3	4.0573	0.0001	4.0573	36.000	35.877	0.0000	0.0000	0.0696	0.0718
0.7981	0.0568	2677.8	8.1146	0.0001	8.1145	36.000	35.504	0.0000	0.0000	0.1910	0.1956
0.7087	0.1079	2378.1	15.4253	1.4292	13.9961	35.900	34.503	0.1976	0.0619	0.3771	0.2909
0.6206	0.1353	2082.5	19.3356	2.8583	16.4774	35.597	33.907	0.4570	0.1421	0.4524	0.3657
0.4294	0.1701	1440.8	24.3154	4.2724	20.0430	35.093	32.856	1.0000	0.3064	0.7086	0.5205
CASE II											
0.3555	0.1768	1193.0	25.2535	4.4153	20.8382	35.093	32.585	0.9386	0.3676	0.7445	0.5788
0.2478	0.1826	831.6	26.0934	4.5582	21.5353	34.966	32.343	0.8503	0.4550	0.9182	0.6639
0.2347	0.1830	787.6	26.1544	4.5725	21.5819	34.959	32.326	0.8397	0.4555	0.9330	0.6743
0.2208	0.1834	740.8	26.2097	4.5868	21.6230	34.952	32.312	0.8284	0.4768	0.9467	0.6853
0.2058	0.1837	690.7	26.2586	4.6010	21.6576	34.946	32.299	0.8164	0.4887	0.9655	0.6972
0.1897	0.1840	636.4	26.2994	4.6153	21.6840	34.939	32.290	0.8035	0.5015	0.9835	0.7100
CASE III											
0.1719	0.1842	576.9	26.3301	4.6296	21.7005	34.932	32.284	0.7893	0.5157	0.9977	0.7241
0.1162	0.1847	389.8	26.3963	4.6654	21.7309	34.916	32.273	0.7449	0.5600	0.9932	0.7683
0.1090	0.1848	365.8	26.4029	4.6689	21.7340	34.914	32.271	0.7392	0.5657	0.9475	0.7740
0.1014	0.1848	340.2	26.4096	4.6725	21.7371	34.912	32.270	0.7331	0.5717	0.9414	0.7801
0.0931	0.1848	312.5	26.4162	4.6761	21.7401	34.911	32.269	0.7265	0.5783	0.9348	0.7866
0.0841	0.1849	282.1	26.4227	4.6796	21.7431	34.909	32.268	0.7193	0.5855	0.9276	0.7938
0.0739	0.1849	247.9	26.4295	4.6832	21.7462	34.907	32.267	0.7112	0.5935	0.9195	0.8019
0.0621	0.1850	208.2	26.4361	4.6868	21.7493	34.906	32.266	0.7018	0.6030	0.9101	0.8113
0.0474	0.1850	159.0	26.4426	4.6904	21.7523	34.904	32.265	0.6901	0.6147	0.8984	0.8230
0.0252	0.1851	84.7	26.4493	4.6939	21.7554	34.902	32.264	0.6725	0.6323	0.8807	0.8406

REFERENCES

1. Heller, S.R. Jr., Brock, J.S. and Bart, R., "The Stresses Around a Rectangular Opening with Rounded Corners in a Beam Subjected to Bending with Shear", Proceedings, Vol. 1, Fourth U.S. National Congress on Applied Mechanics, Berkeley, California, 1962.

2. Bower, J.E., "Elastic Stresses Around Holes in Wide Flange Beams", Journal of the Structural Division, ASCE, Vol. 92, No. ST2, Proc. Paper 4773, April 1966.

3. Bower, J.E., "Experimental Stresses in Wide Flange Beams with Holes", Journal of the Structural Division, ASCE, Vol. 92, No. ST5, Proc. Paper 4945, October 1966.

4. McCutcheon, J.O., Dickie, J.F. and Cheng, S.Y., "Experimental Investigation of Large Extended Openings in the Webs of Wide Flange Beams", McGill University, Applied Mechanics Series No. 6, April 1965.

5. McCutcheon, J.O., So, W-C. and Gersovitz, B., "A Study of the Effects of Large Circular Openings in the Webs of Wide Flange Beams", McGill University, Applied Mechanics Series No. 2, November 1963.

6. Segner, E.P. Jr., "Reinforcement Requirements for Girder Web Openings", Journal of the Structural Division, ASCE, Vol. 90, No. ST3, Proc. Paper 3919, June 1964.

7. Redwood, R.G. and McCutcheon, J.O., "Beam Tests with Unreinforced Web Openings", Journal of the Structural Division, ASCE, Vol. 94, No. ST1, Proc. Paper 5706, January 1968.

8. Bower, J.E., "Ultimate Strength of Beams with Rectangular Holes", Journal of the Structural Division, ASCE, Vol. 94, No. ST6, Proc. Paper 5982, June 1968.

9. Redwood, R.G., "Plastic Behavior and Design of Beams with Web Openings", Proceedings of the Canadian Structural Engineering Conference, Canadian Institute of Steel Construction, Toronto, Feb. 1968.

10. Redwood, R.G., "The Strength of Steel Beams with Unreinforced Web Holes", Civil Engineering and Public Works Review, Vol. 64, No. 755, London, June 1969.

11. Congdon, J.G., "Ultimate Strength of Beams with Reinforced Rectangular Openings", M. Eng. Thesis, McGill University, July 1969.

12. Bower, J.E., "Analysis and Experimental Verification of Steel Beams with Unreinforced Web Openings", Paper prepared for the University of Wisconsin Institute, "Design of Beams with Web Openings", Milwaukee, Wisconsin, January 1970.

13. Frost, R.W., Unpublished Data, U. S. Steel Corporation, Applied Research Laboratory, Monroeville, Pennsylvania.

14. Seeley, F.B. and Smith, J.O., Advanced Mechanics of Materials, New York: John Wiley and Sons, Inc., 1966.

15. "Manual of Steel Construction", American Institute of Steel Construction, Inc., New York, 1970.

ACKNOWLEDGEMENTS

The author wishes to express his sincere appreciation to his major professor, Dr. Peter B. Cooper, without whose assistance and continuing encouragement this thesis would not have been possible.

A word of thanks is extended to Mr. R. W. Frost, U. S. Steel Corporation who provided the available experimental data for comparison purposes.

Appreciation is extended to Kansas State University for the unlimited use of computer facilities. Initial programming and debugging was done on the IBM 1620 Computer and final programs were run on the IBM 360-50 Computer, both at the University Computing Center.

A debt of gratitude is due the author's wife, Sharon, whose patience, understanding and encouragement contributed much toward the successful completion of this thesis.

ULTIMATE STRENGTH ANALYSIS OF BEAMS WITH ECCENTRIC RECTANGULAR WEB OPENINGS

by

MICHAEL WAYNE RICHARD

B. S., United States Military Academy, 1964
B. S., Kansas State University, 1970

AN ABSTRACT OF A MASTER'S THESIS

submitted in partial fulfillment of the

requirements for the degree

MASTER OF SCIENCE

Department of Civil Engineering

KANSAS STATE UNIVERSITY
Manhattan, Kansas

1971

ABSTRACT

A new analytical method of determining the moment carrying capacity of beams with eccentric rectangular web openings is developed. Using this method, the effects of varying the opening eccentricity, length and height were investigated analytically for a number of beam sections. From this analysis, the following conclusions are drawn: a. As opening eccentricity increases, the moment carrying capacity decreases for low shear values and increases for high shear values; b. As opening length increases, the moment carrying capacity decreases; c. As opening height increases, the moment carrying capacity decreases; d. As opening length becomes successively smaller than opening height, the moment carrying capacity increases; e. Shear forces are unequally distributed across unequal web areas above and below eccentric openings. The larger area carries the larger shear force.

The analytical results compared favorably with the limited experimental data available. In all cases, the analytical results were slightly conservative.